Factors controlling nitrate fluxes in groundwater in agricultural areas

Lixia Liao,[1] Christopher T. Green,[1] Barbara A. Bekins,[1] and J. K. Böhlke[2]

Received 5 June 2011; revised 21 November 2011; accepted 30 December 2011; published 24 February 2012.

[1] The impact of agricultural chemicals on groundwater quality depends on the interactions of biogeochemical and hydrologic factors. To identify key processes affecting distribution of agricultural nitrate in groundwater, a parsimonious transport model was applied at 14 sites across the U.S. Simulated vertical profiles of NO_3^-, N_2 from denitrification, O_2, Cl^-, and environmental tracers of groundwater age were matched to observations by adjusting the parameters for recharge rate, unsaturated zone travel time, fractions of N and Cl^- inputs leached to groundwater, O_2 reduction rate, O_2 threshold for denitrification, and denitrification rate. Model results revealed important interactions among biogeochemical and physical factors. Chloride fluxes decreased between the land surface and water table possibly because of Cl^- exports in harvested crops (averaging 22% of land-surface Cl^- inputs). Modeled zero-order rates of O_2 reduction and denitrification were correlated. Denitrification rates at depth commonly exceeded overlying O_2 reduction rates, likely because shallow geologic sources of reactive electron donors had been depleted. Projections indicated continued downward migration of NO_3^- fronts at sites with denitrification rates <0.25 mg-N L^{-1} yr^{-1}. The steady state depth of NO_3^- depended to a similar degree on application rate, leaching fraction, recharge, and NO_3^- and O_2 reaction rates. Steady state total mass in each aquifer depended primarily on the N application rate. In addition to managing application rates at land surface, efficient water use may reduce the depth and mass of N in groundwater because lower recharge was associated with lower N fraction leached. Management actions to reduce N leaching could be targeted over aquifers with high-recharge and low-denitrification rates.

Citation: Liao, L., C. T. Green, B. A. Bekins, and J. K. Böhlke (2012), Factors controlling nitrate fluxes in groundwater in agricultural areas, *Water Resour. Res.*, *48*, W00L09, doi:10.1029/2011WR011008.

1. Introduction

[2] Nitrate (NO_3^-) is one of the most abundant contaminants in groundwater, with potentially harmful effects on human and environmental health. Substantial groundwater pollution has resulted from agricultural systems with large inputs of fertilizers and irrigation water [*Hallberg*, 1986; *Burt et al.*, 1993; *Böhlke*, 2002; *Hatfield and Follett*, 2008; *Dubrovsky et al.*, 2010], and further intensification of agricultural practices is likely given population growth and a new interest in biofuel crops to meet energy needs [*110th United States Congress*, 2007]. To balance intense agricultural demands against the costs of degraded water quality requires understanding of the hydrogeochemical processes in soils and aquifers that determine the effects of agricultural practices on water quality. In the unsaturated zone, hydrologic conditions and complex soil processes control the fraction of applied nitrogen on land surface that leaches to the water table. Below the water table, the fate of NO_3^- is further affected by physical and chemical processes. The interactions of these various factors make some aquifers more vulnerable to NO_3^- contamination than others [*Evans and Maidment*, 1995; *Nolan and Hitt*, 2006; *Debernardi et al.*, 2008]. Although many of the processes controlling NO_3^- movement in the subsurface are understood, applications of deterministic models integrating hydrology, geochemistry, and changing agricultural practices across multiple diverse settings are relatively scarce. Such tools could be useful for developing effective agricultural practices and meeting sustainable water quality goals.

[3] Agricultural nitrogen (N) inputs at land surface have long been recognized as a substantial factor in N contamination of groundwater. *Pionke and Urban* [1985] reported that NO_3^- concentrations in groundwater underlying cropland were five to seven times those observed in areas underlying forests in a small Pennsylvania watershed. During the last 50 yr, agricultural inputs of N have increased 20-fold, and concentrations in groundwater have risen concurrently [*Hallberg*, 1986; *Böhlke and Denver*, 1995; *Böhlke*, 2002; *Puckett et al.*, 2011]. Effects of agricultural inputs, however, vary depending on site conditions. The fraction of applied N that leaches to groundwater as NO_3^- ranges from ~5% to 50%, depending on local conditions [*Hallberg*, 1986; *Johnes*, 1996; *Böhlke*, 2002; *Tesoriero et al.*, 2007; *Green et al.*, 2008a; *Zhang and Hiscock*,

[1]National Research Program, U. S. Geological Survey, Menlo Park, California, USA.
[2]National Research Program, U. S. Geological Survey, Reston, Virginia, USA.

This paper is not subject to U.S. copyright.
Published in 2012 by the American Geophysical Union

2010; *Puckett et al.*, 2011] and uptake by harvested crops can be up to 50% [*Cassman et al.*, 2002]. Many studies have indicated that the likelihood of NO_3^- contamination is greater in shallow aquifers with high N loading and well-drained surficial soil [e.g., *Spalding and Exner*, 1993; *Nolan et al.*, 2002].

[4] The fate and transport of NO_3^- in groundwater depends on physical processes (e.g., recharge and application rates) and geochemical conditions (mineral composition and redox processes) within the saturated zone. Greater recharge rates lead to more rapid vertical transport of NO_3^- into deeper zones. At the same time, the application of low-N irrigation water can cause dilution of N concentrations in groundwater [*Nolan and Hitt*, 2006; *Debernardi et al.*, 2008]. Near the bottom of the aquifers, impermeable zones may inhibit vertical water movement and decrease the rate of vertical migration of NO_3^-. In addition to these physical factors, natural attenuation due to denitrification can diminish the vertical flux of NO_3^-. For many sites, it is difficult to ascertain whether the observed depth of NO_3^- contamination results from the influence of denitrification or from physical factors that have limited the vertical migration of NO_3^- from agricultural sources. Clearly, models of agricultural effects on groundwater quality must account for the combined effects of hydrological and chemical factors on NO_3^- fluxes in aquifers.

[5] Removal of NO_3^- from groundwater by denitrification, a microbiological process by which NO_3^- is converted to N_2, largely depends on geochemical conditions in aquifers. Under oxic conditions, dissolved O_2 is used preferentially by subsurface microorganisms as an electron acceptor and denitrification is inhibited. Typically, evidence of denitrification is found in groundwater samples with low O_2 concentrations (e.g., <2 mg L^{-1}, although actual inhibition levels at reaction sites may be lower) [*Green et al.*, 2008b., 2010]. Combined use of groundwater dating and dissolved gas analysis of N_2 produced by denitrification has allowed the estimation of denitrification rates in many groundwater systems [*Vogel et al.*, 1981; *Böhlke and Denver*, 1995; *Böhlke et al.*, 2002; *McMahon et al.*, 2004a, 2008b; *Singleton et al.*, 2009; *Tesoriero et al.*, 2007]. Substantial denitrification has been observed in aquifers containing relatively young groundwater (with travel times of years to decades) [*Postma et al.*, 1991; *Böhlke et al.*, 2002, 2007b], while no evidence of denitrification has been observed in other, much older groundwater (with travel times of the order of millennia) [*Vogel et al.*, 1981; *McMahon et al.*, 2004b]. The lack of uncertainty analyses in most of these previous estimates and the wide range and heterogeneity of rates make it difficult to generalize about the influence of denitrification on groundwater quality in the absence of local geochemical information. Difficulties persist in comparing results from multiple aquifers and in determining how denitrification interacts with other factors (e.g., water recharge and N inputs at land surface) affecting N storage and flux in groundwater.

[6] Studies using statistical methods, interpretation of data from field sites, and detailed numerical models have explored relations among factors controlling NO_3^- concentrations in groundwater. Regression models have assessed the probabilities of contamination of aquifers by NO_3^- at various scales [*Eckhardt and Stackelberg*, 1995; *Evans and Maidment*, 1995; *Tesoriero and Voss*, 1997; *Nolan et al.*, 2002; *Nolan and Hitt*, 2006; *Burow et al.*, 2010]. Application rates of N, water input, and soil texture were generally identified as important factors influencing N concentrations in groundwater. However, these statistical methods provide limited information about the mechanisms controlling N concentration and their spatial distribution within groundwater. Many field studies have documented mechanisms affecting N in groundwater [e.g., *Postma et al.*, 1991; *Böhlke and Denver*, 1995; *Böhlke et al.*, 2002; *Tesoriero et al.*, 2007; *Green et al.*, 2008a]. For example, *Green et al.* [2008a] identified N application rate, water input, and evapotranspiration as major factors controlling the N fluxes in groundwater. *Böhlke and Denver* [1995] emphasized the interactive effects of changing agricultural practices, groundwater residence times, and local geologic features on NO_3^- transport and mass balance in local flow systems. Several recent studies have synthesized results among many sites using consistent methods in order to study broad scale trends in recharge [*McMahon et al.*, 2011], relations between applied N and N in recharge [*Puckett et al.*, 2011], and reaction rates [*Tesoriero and Puckett*, 2011]. More work is needed to address these multiple factors simultaneously in a consistent hydrologic framework with physical and chemical processes in saturated and unsaturated zones. Detailed numerical groundwater models have been applied to study factors relevant to N contamination such as source area distributions [*McMahon et al.*, 2008a; *Starn et al.*, 2010], travel times [*Weissmann et al.*, 2002], and redox reactions [*Frind et al.*, 1990; *Wriedt and Rode*, 2006; *Green et al.*, 2010; *Kauffman and Chapelle*, 2010]. Detailed numerical transport models have been effective for studying processes and making predictions at individual sites, but are typically too complex and difficult to implement in a consistent manner for timely analysis of broad differences among many sites [*Konikow*, 2011]. Relatively few studies have evaluated NO_3^- fluxes from land surface through aquifers using consistent methods applied across a wide range of hydrological and geochemical settings. A relatively simple transport model that synthesized multiple chemical profiles was developed recently to assess various controlling factors of vertical N fluxes in shallow groundwater in northwestern Mississippi [*Welch et al.*, 2011]. This model accounts for the physical and chemical factors of interest for N fluxes in groundwater, allows automatic parameter estimation and predictions with uncertainty analysis, and can be applied quickly to multiple sites. In addition to NO_3^-, the model considers fluxes of chloride (Cl^-), which is commonly enriched in groundwater affected by agriculture, and which can serve as an indicator of nonreactive solute transport.

[7] The objectives of the current study were to further develop the simple flux model of *Welch et al.* [2011] and test it in 14 aquifers in different hydrogeologic settings across the USA; to use calibrated model results to identify which physical and chemical factors control vertical N fluxes in groundwater under a wide range of conditions; and to generalize the influence of these factors on long-term aquifer vulnerability. These results will improve scientific understanding of interrelations among the physical and chemical factors that control N fluxes across a wide range of sites and will clarify land-use management options best suited to controlling N contamination.

2. Site Descriptions

[8] To evaluate the applicability of our model for assessing impacts of agricultural practices on nitrogen fluxes in groundwater, 14 study sites (Table 1) were selected from the U. S. Geological Survey (USGS) National Water Quality Assessment (NAWQA) program and other previous studies with suitable data. Data sets at each site typically included concentrations of dissolved gases (oxygen, argon, nitrogen), Cl^-, NO_3^-, and environmental tracers of groundwater age (tritium, chlorofluorocarbons [CFCs], and SF_6), later referred to as "age tracers." Sample locations were chosen from recharge areas at all of the sites. Samples from areas of low topography or near gaining surface water bodies were excluded to avoid discharge areas affected by upward groundwater fluxes. Samples in, or near, perched water tables were also excluded. Figure 1 shows the locations of the 14 study areas in Merced County, California (CA), Hardin County, Iowa (IA), Kent County, Maryland near Kennedyville (MD/K) and Locust Grove (MD/L), Anne Arundel County, Maryland (MD/A), Sherburne County, Minnesota (MN), Bolivar County, Mississippi (MS), Scotts Bluff and Sioux Counties, western-Nebraska (NE/W), Colfax County, eastern-Nebraska (NE/E), Yakima County, Washington (WA), Portage County, Wisconsin (WI), Greene County, North Carolina (NC), Carson County, Texas (TX), and Suffolk County, New York (NY). The relevant publications used in this study for each site are listed in Table 1. The CA, NE/E, MD/K, WA, IA, and MS sites are from USGS NAWQA studies. The IA site was sampled in the same manner as the CA, WA, MD/K, and NE/E sites, as described in the work of *Green et al.* [2008b]. The sampling of the remaining sites is described in the cited publications. The study sites have unsaturated zones with depths from 3 to 100 m. Saturated thicknesses of the aquifers range from several meters to 100 m. Climates range from arid/semiarid at the western sites (e.g., WA and CA) to humid continental in the midcontinent (e.g., NE) and humid subtropical in the eastern (e.g., MD) sites, with precipitation rates of 0.19–1.14 m yr^{-1} (Table 1). The quantities of nitrogen applied on the land surface varied substantially among sites (estimates for 2001 are summarized in Table 2) and were derived from chemical fertilizer, manure, irrigation water, and atmospheric nitrogen loadings, as explained in section 3. Among the studied sites, corn, soybean, and pasture were common crops, accompanied by smaller acreages of a wide variety of crops including orchards, hay, alfalfa, grapes, vegetables, wheat, and potatoes.

3. Model Implementation and Calibration

[9] In this study, a previously developed mathematical model [*Welch et al.*, 2011] was expanded to estimate the vertical transport of multiple reactive and conservative solutes through the studied aquifers. The expanded model includes age tracers, O_2 transport, and inhibition of denitrification by O_2. As before, the vertical flow component and associated travel time to a given depth were based on an idealized two-dimensional conceptual model of a water table aquifer with an underlying confining unit (Figure 2). The model parameters were recharge rate, unsaturated zone travel time, fractions of N and Cl^- inputs leached to groundwater, O_2 reduction rate, O_2 threshold for denitrification, and denitrification rate. These parameters were estimated by simultaneously fitting observations of multiple environmental tracers consisting of NO_3^-, excess N_2 (N_2 from denitrification), O_2, Cl^-, and age tracers. Additional details and mathematics of the vertical flux and reaction model are described below, followed by an explanation of the procedure for estimating model parameters.

[10] For a solute, i, a fraction (f_i) of the mass applied at land surface (M_i) is transported through the unsaturated zone to the water table. Chemical and physical processes removing solute mass in the unsaturated zone are not modeled mechanistically, but are accounted for in the parameter f_i. For example, denitrification in soils reduces the value of f_N, the fraction of applied N that reaches the water table as NO_3^-. Based on previous studies, we expect that NO_3^- is the dominant form of N reaching the water table at agricultural sites [*Green et al.*, 2008a]. The nonleaching fraction (1-f_N) also includes other N losses such as export in harvested crops, which could be up to 50% of applied N [*Cassman et al.*, 2002], or by runoff to surface water including through tile drains. The use of a leaching fraction parameter has been applied widely in the U.S. [e.g., *Puckett et al.*, 2011] and the U.K. [e.g., *Zhang and Hiscock*, 2010]. Below the water table, solutes travel through the saturated zone and the concentration (C_i) of solutes can be monitored with time (t) and depth (z). In the modeled saturated zone, O_2 reduction commences at the water table. Inhibition of denitrification by O_2 and the onset of denitrification at depth were constrained by the observed distributions of O_2 and excess N_2. The parsimonious model allows for efficient calibration, consistent assessment of N fluxes at multiple sites with different hydrological and geological settings, evaluation of nonlinear model uncertainties, and prediction of future groundwater quality. The simplifying assumptions of the model (e.g., spatially uniform chemical and water applications at land surface at each site) are consistent with study sites in recharge areas of dominantly agricultural regions. The concentration of a solute at a particular depth below the water table and time is given by:

$$C_i(t,z) = \frac{M_i(t')f_i}{R} - (\tau_{s_i} - \tau_{\mathrm{lag}_i})k_i, \tag{1}$$

$$\tau_{\mathrm{lag}_N} = (C_{O_0} - C_{O_{cut}})/k_O,\ \tau_{\mathrm{lag}_O} = 0, \tag{2}$$

where C_i (t, z) is the concentration [M/L^3] of solute, i, at time, t, and depth, z [L]; $M_i(t')$ is the spatially uniform mass flux [M/L^2/T] of solute, i, at the ground surface at the time of application, t'; f_i is the fraction of the applied mass reaching the water table; R is the recharge [L/T]; k_i is the zero order reaction rate [M/L^3/T] (k_O for O_2 reduction rate and k_N for denitrification rate) in the saturated zone; τ_s is the saturated zone travel time; τ_{lag_N} for NO_3^- is the time lag between recharge and the onset of denitrification; C_{O_0} is recharge concentration of O_2 at the water table; and $C_{O_{cut}}$ is the threshold concentration of O_2 above which denitrification does not occur. Reactions of O_2 in the unsaturated zone are not modeled explicitly, but are accounted for by calibrating the concentration of O_2 at the water table (C_{O_0}) from data at each site. The reaction kinetics of O_2 reduction and denitrification are uncertain because of limited information

Table 1. Characteristics of Studied Sites

Site Name, State and County	Sampling Date	Sedimentary Geology (From Shallow to Deep)	Climate	Crop in Source Area	Precipitation (m yr^{-1})	Irrigation (m yr^{-1})	Soil Texture[a]	Drainage Class	Reference
TX Texas (Carson)	August–November, 1994	(A) Playa with vertisolic Randall clay soil (B) lacustrine deposits of a heterogeneous mud and sands	Humid subtropical	Corn, wheat, sorghum and cotton	0.57	0.43	Clay	Poorly drained	[*Fryar et al.*, 2000]
MD/L Maryland (Kent)	May–September, 1991	(A) Sand and gravel of fluvial pennsauken formation (B) clays and silts	Humid subtropical	Pastures, nurseries, corn and soybeans	1.12	0	Silt loam	Well drained	[*Böhlke and Denver*, 1995]
NY New York (Suffolk)	January, 2007	(A) Moraine and outwash sand and gravel with local silt and clay (B) glacial-lake clay, silt, and sand	Humid subtropical	Turf grass, corn, grapes, and potatoes	1.14	0	Loam and loamy sand	Well drained	[*Böhlke et al.*, 2009]
WI Wisconsin (Portage)	June, 2004	(A) Glacial and fluvial deposits overlying crystalline bedrock	Humid continental	Corn, forage, and vegetables	0.76	0.40	Sandy loam	Well drained	[*Tesoriero et al.*, 2007]
MD/K Maryland (Kent)	April–October, 2004	(A) Thin layer of quartz sands and gravels (B) coarsening upward muddy glauconitic sand	Humid subtropical	Corn, soybeans, small grain, pastures, hay	1.12	0	Sandy loam	Well drained	[*Green et al.*, 2008b]
NE/W Nebraska (Scotts Bluff)	August, 1998	(A) Unconsolidated sand and gravel alluvium (B) consolidated sedimentary bedrock	Humid continental	Hay, corn, wheat, and dry beans	0.34	0.89	Loamy fine sand to fine sandy loam	Well drained to excessively drained	[*Böhlke et al.*, 2007a]
WA Washington (Yakima)	April–October, 2004	(A) Sandy silt dissected by subvertical clastic dikes (B) loess, debris flows, alluvium, colluviums, and fluvial sands and cobbles	Arid	Corn, pasture, grapes, asparagus,	0.19	0.74	Silt loam	Well drained	[*Green et al.*, 2008b]
NC N. Carolina (Greene)	April, 2003	(A) Sandy, clayey silt (B) gravelly sands and a phosphatic gravelly, shelly sand	Humid subtropical	Corn and soybean	0.95	0.18	Fine sandy loam	Poorly drained mixed moderately well drained	[*Tesoriero et al.*, 2007]
CA California (Merced)	April–Oct, 2004	(A) Thin unsaturated, eolian sands (B) alluvial sands, silts, and clays (C) lacustrine clay	Arid to semiarid	Orchards, corn, vegetables	0.31	1.20	Sand	Somewhat excessively drained	[*Green et al.*, 2008b]
MN Minnesota (Millelacs)	August, 1993	(A) Outwash sand (B) sand-plain aquifer with silt and clay rich glacial till	Humid continental	Alfalfa and corn	0.70	0.49	Fine sandy loam and loam fine sandy	Mixed with poorly drained and well drained	[*Böhlke et al.*, 2002]
MS Mississippi (Bolivar)	June, 2008	(A) 3 to 30 m thick silts and clays (b) sand and gravel layer	Humid subtropical	Cotton, corn, rice, sorghum, and soybeans	0.93	0.41	Silt clay	Poorly drained	[*Welch et al.*, 2011]

Table 1. (continued)

Site Name, State and County	Sampling Date	Sedimentary Geology (From Shallow to Deep)	Climate	Crop in Source Area	Precipitation ($m\ yr^{-1}$)	Irrigation ($m\ yr^{-1}$)	Soil Texture[a]	Drainage Class	Reference
MD/A Maryland (Anne Arundel)	April, 1996	(A) Fine-grained sand and diatomaceous silt (B) fine sand and silt with a large fraction of glauconite	Humid subtropical	Corn and forest	1.14	0	Silt loam	Poorly drained	[*Böhlke et al.*, 2007b]
IA Iowa (Hardin)	August, 2007	(A) Unconsolidated silt, sand and gravel (B) glacial till	Humid continental	Corn and soybean	0.65	0.15	Loam to silt clay loam	Mostly poorly drained with some well drained	
NE/E Nebraska (Colfax)	April–October, 2004	(A) Unsaturated loess (B) terraced sand and gravel deposits	Humid continental	Corn, soybeans, alfalfa, pasture	0.72	0.20	Loam to silt loam	Poorly drained	[*Green et al.*, 2008b]

[a]Soil texture data are from USDA national soil survey database (available at http://websoilsurvey.nrcs.usda.gov/app/HomePage.htm). Soil drainage classes were assigned using the USDA National Soil Survey Handbook (available at http://soils.usda.gov/technical/handbook/contents/part618.html).

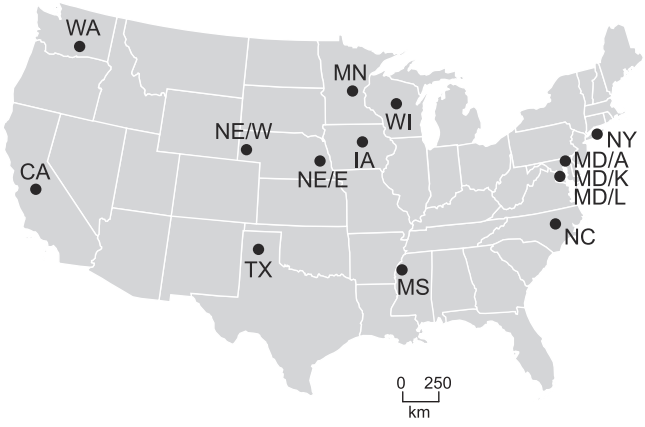

Figure 1. Locations of 14 studied sites.

about the possible rate-limiting effect of electron donors, spatial heterogeneity, and/or limited vertical resolution at the various sites. Zero-order degradation was assumed for our kinetic models. At most sites, data were not sufficient to distinguish reliably between different rate laws; however, in a direct comparison at two sites with relatively well-defined vertical profiles of O_2 (MN and WI), zero-order models gave smaller sum-of-square errors (by 1%–27%) than first-order models for the reactive species O_2, NO_3^-, and N_2. The model does not account for potential depletion of electron donor phases in the aquifers. Specific abundances and rate controls of redox-reactive phases typically are poorly known and long-term projections would benefit from improvements in their characterization.

[11] The sample time, t, and application time, t', are related by

$$t' = t - \tau_u - \tau_s, \tag{3}$$

where τ_u is the unsaturated zone travel time and τ_s is the saturated zone travel time. The unsaturated zone travel time τ_u is estimated with:

$$\tau_u = \frac{n_u H_u}{R}, \tag{4}$$

where n_u is the unsaturated zone mobile water content [L^3/L^3], which is the specific volume through which the unsaturated zone water is transported, and H_u is the unsaturated zone thickness [L]. Use of n_u or τ_u in model calibration yields identical predictions because these parameters are directly proportional. The saturated zone travel time is estimated for a homogeneous aquifer of uniform thickness with [*Vogel*, 1967]:

$$\tau_s = \frac{n_s H_s}{R} \ln\left(\frac{H_s}{H_s - z}\right), \tag{5}$$

where n_s is the saturated mobile water content (assumed to be equal to the porosity), H_s is the saturated zone thickness, and z is the depth of the sample point below the water table.

[12] Values of mass flux of N at the ground surface (M_N) were based on county-level estimates of sources including fertilizer, atmospheric deposition, manure, and N in irrigation

Table 2. Fixed and Predicted Parameter Values From Vertical Transport Model

Parameters	TX	MD/L	NY	WI	MD/K	NE/W	WA	NC	CA	MN	MS	MD/A	IA	NE/E
	Low k_N						Medium k_N			High k_N				
Fixed Values[a]														
Aquifer porosity, n_s	0.45	0.40	0.30	0.30	0.32	0.35	0.30	0.40	0.38	0.40	0.33	0.50	0.40	0.37
Aquifer thickness, H_s (m)	100	21	37	50	16	80	100	50	31	12	41	15	30	31
Depth to water, Z (m)	100	3	20	30	8	5	7	3	7	5	8	3	3	22
Nitrogen application rates in 2001, M_N (kg ha^{-1} yr^{-1})	87.8	154	159	113	154	164	168	215	215	56.7	73.2	151	94.0	114
Calibrated Parameters														
Recharge rate, R (m yr^{-1})	0.01	0.31	0.59	0.11	0.14	0.57	0.17	0.12	0.38	0.10	0.07	0.06	0.16	0.08
N leaching fraction, f_N	0.02	0.30	0.29	0.20	0.11	0.25	0.25	0.13	0.60	0.12	0.10	0.04	0.11	0.19
Cl^- leaching Fraction, f_{Cl}	0.64	1.29	NE[b]	0.29	0.69	0.69	0.48	0.79	0.93	0.25	0.26	0.38	1.02	0.22
Unsaturated zone mobile water content (n_u)	0.00	0.31	0.05	0.09	0.03	0.13	0.08	0.12	0.38	0.13	0.01	0.10	0.15	0.06
Recharge concentration of O_2, C_{O_0} (mg L^{-1})	10.0	8.99	8.63	9.25	9.26	6.38	5.23	8.55	5.71	10.0	9.27	8.65	5.57	9.26
Threshold concentration of O_2, $C_{O_{cut}}$ (mg L^{-1})	NE	NE	NE	NE	NE	6.16	5.23	8.55	5.71	3.93	0.61	2.01	3.64	5.19
Denitrification rate, k_N (mg-N L^{-1} yr^{-1})	NE	NE	NE	NE	NE	0.01	0.04	0.17	0.20	0.27	0.36	0.88	1.67	1.93
Oxygen reaction rate, k_O (mg-O_2 L^{-1} yr^{-1})	0.00	0.00	0.00	0.07	0.12	0.15	0.20	0.37	0.64	0.62	0.76	0.67	1.18	0.89
Derived Values														
RRMSE (relative root-mean-square error)	0.71	0.22	0.68	0.47	0.64	0.73	0.85	0.71	0.57	0.49	0.15	0.11	1.20	2.22
Unsaturated zone travel time, τ_u (yr)	32.6	1.65	2.46	33.0	1.47	1.03	3.19	3.03	6.55	6.00	1.16	4.53	2.32	15.9
Saturated zone mean travel time, $\overline{\tau}_s$ (yr)[c]	3725	27	24	135	36	49	178	162	31	47	205	114	77	161
Depth of NO_3^- extinction at present, Z_{curr} (m)	2	20	34	17	13	60	34	15	25	5	5	2	2	3
Depth of NO_3^- extinction at steady state, Z_{ss} (m)	100	21	37	50	16	80	97	28	31	6	7	3	2	3
Time required to reach steady state (yr)	25,800	197	162	952	245	54	572	354	113	35	27	26	1.5	30
meq ratio (k_N/k_O)	NE	NE	NE	NE	NE	0.20	0.52	1.34	0.88	1.26	1.35	3.77	4.06	6.20

[a]Fixed values are based on data reported in the corresponding literature for each study site.
[b]NE means not estimated for f_{Cl} because of unquantified sources of Cl^-, and for k_N and $C_{O_{cut}}$ because of excess N_2 below detection limits.
[c]Calculated with $\overline{\tau}_s = n_s H_s / R$, where $\overline{\tau}_s$ is mean travel time, n_s is aquifer porosity, H_s is aquifer thickness, and R is recharge [e.g., *Böhlke*, 2002].

water. The fixation of atmospheric N was not included in the source term for these sites. Nitrogen fertilizer mass loadings for 1945–2001 were from previous studies [*Alexander and Smith*, 1990; *Ruddy et al.*, 2006]. Annual manure inputs were based on livestock inventory estimates from the National Agricultural Statistics Service (available at http://www.nass.usda.gov/Statistics_by_State/) and manure nutrient content estimates from *Ground Water Monitoring and Assessment Program* [2001] using methods described in the Agricultural Waste Management Field Handbook [*Soil Conservation Service*, 1992]. Intensity of N inputs from fertilizer and manure (kg ha^{-1}) were calculated by dividing the mass of

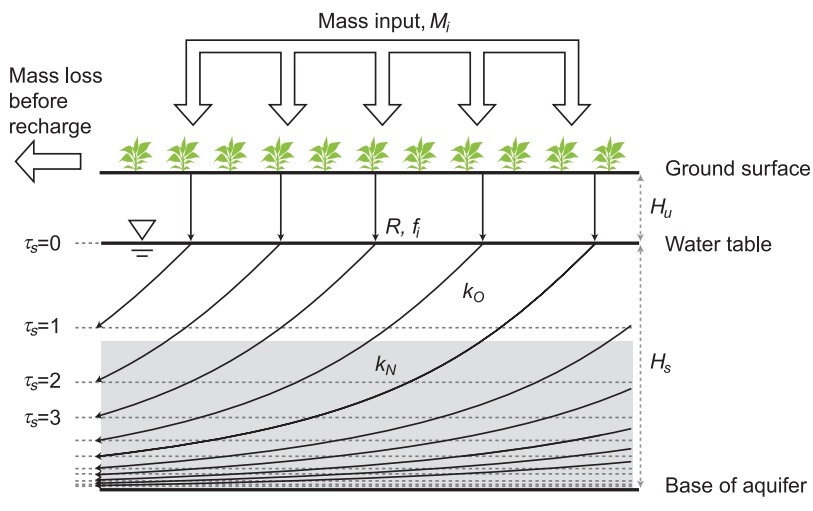

Figure 2. Conceptual model of vertical chemical fluxes in groundwater at a recharge area. M_i, mass applied at land surface, R, recharge rate, f_i, leaching fraction, k_O, oxygen reduction rate, k_N, denitrification rate, H_u, thickness of unsaturated zone, H_s, thickness of saturated zone, and τ_s, saturated zone travel time. The shaded portion of the aquifer is the zone of active denitrification. Solid arrows indicate pathlines for water and solutes. Horizontal dashed lines in the saturated zone indicate isochrons of groundwater travel time since recharge.

N inputs by the area of cropland in the county (available at http://quickstats.nass.usda.gov/). Total annual atmospheric deposition fluxes were derived from Clean Air Status and Trends Network (CASTNET) data including dry and wet deposition at nearby monitoring stations over the time period of available data for each station (available at http://java.epa.gov/castnet/). Loadings of N from all sources were assumed to decrease linearly from levels in 1945 to background levels in 1900, which were assumed equal to the average of total (wet plus dry) atmospheric deposition over the time period of available data for each site.

[13] Chloride was considered to be nonreactive in the subsurface, and the reaction rate, k_{Cl}, was set to zero. Sources of applied Cl^- (M_{Cl}) included fertilizers, atmospheric deposition, irrigation water, and manure. Fertilizer Cl^- application rates were estimated using data from the United States Department of Agriculture (USDA) (available at http://www.ers.usda.gov/Data/FertilizerUse/). Estimated state-level application rates of KCl for various crop types were combined with county-level crop areas from the U.S. Department of Agriculture National Agricultural Statistics Service (available at http://www.nass.usda.gov/Data_and_Statistics/). The long-term average Cl^- flux in atmospheric wet deposition at each site was estimated using the map of interpolated data from the National Atmospheric Deposition Program (NADP) (available at http://nadp.sws.uiuc.edu/). The rate of Cl^- dry atmospheric deposition from CASTNET (available at http://nadp.sws.uiuc.edu/) was typically lower than 0.05 kg ha^{-1} and was not included in flux estimates. Total loadings of Cl^- were assumed to decrease linearly from 1964 levels to background rates in 1900, which were assumed to be equal to the average rate of atmospheric deposition using available data from NADP. Chloride content in manure was estimated from *Ground Water Monitoring and Assessment Program* [2001] using the same method as N input from manure. Chloride sources from irrigation were estimated using the deep groundwater concentrations of Cl^- combined with irrigation rates at the following sites: NE/E, MS, MN, WI, and NC. At NE/W, Cl^- in irrigation originates mainly from surface waters, and concentrations were taken from *Harvey and Sibray* [2001]. At the CA site, locally high rates of Cl^- application on almond orchards were based on fertilizer application rates reported by the landowner. At the NY site, Cl^- loading was not included in the model because of high-Cl^- concentrations possibly from unquantified Cl^- sources such as sea spray and road salt [*Böhlke et al.*, 2009].

[14] Input data for gaseous environmental tracers of groundwater age (e.g., CFC's, SF_6) were adopted from historical atmospheric concentrations [*Busenberg and Plummer*, 1992, 2000]. Data for CFCs were not included in cases where laboratory reports indicated possible degradation of the CFC's. Input data for tritium (^3H) were estimated from concentrations in rainfall reduced by the amount of radioactive decay between the time of rainfall and time of sampling listed in Table 1 for each site. The tritium residence time in the unsaturated zone was included in the model. Tritium input concentration at each site was estimated from existing long-term records using a national interpolation model [*Michel*, 1989], except for the NY site where local estimates were available [*Böhlke et al.*, 2009]. Equations (1)–(5) were used to model age-tracer transport by assuming a reaction rate of zero and a leaching fraction of one. Input of dissolved oxygen (O_2) at the water table was assumed to be constant over time, and the input concentration was calibrated for each site based on observed O_2 concentrations near the water table.

[15] To test for possible effects of dispersion on model calibration, the model was adapted to include Fickian dispersion for the MD/A site. The resulting modeled concentration profiles were smoothed but there was no significant improvement in the model calibration. For simplicity, all temporally varying input functions were smoothed using 5-yr running averages to avoid convergence problems in calibration associated with noisy derivatives, and as an approximation for the effect of dispersion.

[16] Simulated vertical profiles from equations (1)–(5) were matched to observations by adjusting R, f_N, f_{Cl}, k_N, k_O, C_{O_0}, $C_{O_{cut}}$, and n_u. At well screens with data from multiple sample dates, the averages of all samples were used to avoid the effects of seasonal variation. In addition, if data from multiple locations in the recharge zone were available then these were combined into a single profile. In the case of combined profiles, measurements from all depths were used, and no spatial averaging was performed. The concentrations and depths of all observations are provided in Figures 3 and S1–S13. Fixed values were specified for aquifer porosity (n_s), saturated zone thickness (H_s), and unsaturated zone thickness (H_u) based on published data for site (Tables 1 and 2). Parameters were calibrated by minimizing the sum of squared errors (SSE) between measured and modeled concentrations.

$$\mathrm{SSE} = \sum_{j=1}^{m}\sum_{i=1}^{n}\left(\frac{C_{i,j} - C'_{i,j}}{\overline{C}_j}\right)^2, \tag{6}$$

where i is the observation number, j is the observation type, $C_{i,j}$ are observed values, $C'_{i,j}$ are modeled values, $\overline{C}_j$ is an average of observed values of type j, n is the number of observations of type j, and m is the number of observation types, which include age tracers, NO_3^-, excess N_2 (N_2 from denitrification), O_2, and Cl^-. The sum of square errors (SSE) was minimized using a nonlinear generalized reduced gradient solver [*Lasdon et al.*, 1978]. The goodness-of-fit of model predictions to observations was assessed by the relative root-mean-square error (RRMSE) given by the square root of the quantity SSE divided by the number of observations. Model reliability was further evaluated by varying initial values of parameters to check for correlations and nonunique solutions, and by estimating nonlinear simultaneous 95% confidence intervals of parameters of interest [see *Hill and Tiedeman*, 2007; *Welch et al.*, 2011]. As described in section 5, calibrated parameter values then were used with analytical solutions from equations (1)–(5) to assess potential long-term aquifer vulnerability at each site. The steady state depth of NO_3^- penetration and total mass of NO_3^- in groundwater were computed assuming that future inputs continue at the level of 2001 application rates. A sensitivity analysis was performed to evaluate relative effects of the model parameters on the long term predictions of the depth and mass of NO_3^- in the aquifers.

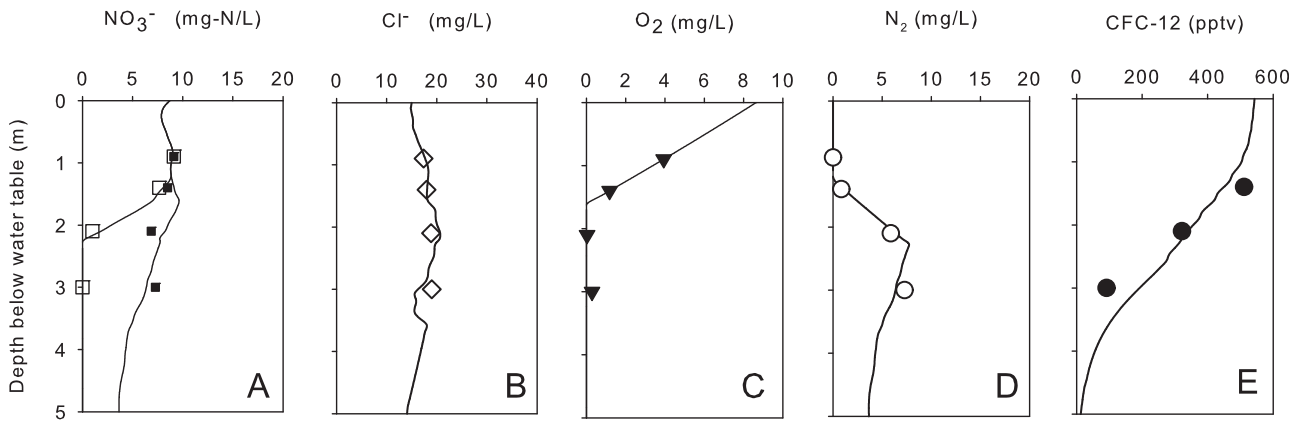

Figure 3. Calibrated vertical transport model results and measured profiles of concentration at site MD/A. (A) NO_3^--N (hollow symbol) and original NO_3^--N in recharge (solid symbol, equal to excess $N_2 + NO_3^--N$), (B) Cl^-, (C) O_2, (D) excess N_2, and (E) age tracers. Samples are from one location and one date. Model parameters are given in Table 2. Similar plots for all sites are given in the Auxiliary Material (Figures S1–S13).[1]

4. Results and Discussion of Calibrated Models

4.1. Estimated Parameters

[17] Overall, the model simulations were able to reproduce the general trends observed in vertical profiles of solute concentrations (Figures 3, S1–S13). The goodness-of-fits of model predictions to observations are listed in Table 2 as relative root-mean-square errors (RRMSE). The estimated parameters including R, f_N, f_{Cl}, k_N, k_O, n_u, and τ_u are listed in Table 2. Recharge rates varied from 0.01 m yr^{-1} at the TX site (in an area with relatively low water inputs and fine-grained surficial soils) to 0.6 m yr^{-1} at the NY site (in an area with abundant precipitation and sandy soils) and the NE/W site (with a large amount of irrigation and leakage from canals). The estimated recharge rates from the vertical flux models of the 14 sites are comparable to estimates from previous studies at those sites (Table S1), which were estimated by the methods of water table fluctuation, stream hydrograph separation, chloride mass balance, and saturated zone age tracers. Discrepancies appear to be most commonly associated with the water table fluctuation method, which may not represent the same spatial or temporal scales of recharge as the saturated zone age tracers used in the present study [e.g., *Delin et al.*, 2000; *Böhlke et al.*, 2007a; *Healy*, 2010; *McMahon et al.*, 2011].

[18] The leaching fractions (f_i) for N and Cl^- are defined as the ratio of mass reaching the water table to that applied at land surface. Values of f_N had a mean of 0.19 and ranged from 0.02 to 0.6, similar to values estimated previously for agricultural sites [*Hallberg*, 1986; *Johnes*, 1996; *Böhlke*, 2002; *Tesoriero et al.*, 2007; *Green et al.*, 2008a; *Zhang and Hiscock*, 2010; *Puckett et al.*, 2011]. Values of f_{Cl} had a mean of 0.61 and ranged from 0.22 to 1.29. At all sites, values of f_{Cl} were higher than values of f_N. This is consistent with the general expectation that chloride moves conservatively in the subsurface [*Herczeg and Edmunds*, 1999], whereas N is subject to a series of transformations and chemical, physical, and biological processes in the unsaturated zone (e.g., plant uptake, denitrification, and volatilization) that tend to reduce its concentration before leaching to the water table. Variability of model f_{Cl} values may point to errors in estimates of local mass application rates of Cl^-, additional processes affecting the Cl^- mass balance at some sites, or uncertainty in the parameter estimates. Values of $f_{Cl} > 1$ at MD/L and IA could result from unaccounted sources of Cl^- such as road salt or irrigation return flow, or underestimates of local Cl^- applications based on county-level fertilizer data. Values of $f_{Cl} < 1$ at the remaining 11 sites could be due to overestimation of local Cl^- inputs or to harvest and removal of crops with accumulated Cl^-. To test the hypothesis that f_{Cl} estimates were affected by Cl^- exports in harvested crops, the estimated losses of Cl^- between ground surface and the water table were compared to independent estimates of Cl^- uptake and export in harvested crops. Literature values for Cl^- concentrations and yields for different crops (see the references in Table S2) were used to estimate Cl^- exports in crops at each study site. Estimated Cl^- exports in harvested crops at the study sites ranged from ~6 to 39 kg ha^{-1} yr^{-1} (Table S3). At a majority of sites with $f_{Cl} < 1$, the estimated values of exported Cl^- in harvested crops were similar to the differences between Cl^- input and Cl^- flux at the water table (Table S3 and Figure 4). For these sites, the results indicate that Cl^- exports in harvested crops may influence f_{Cl} values and are therefore important to consider, for example, when using Cl^- mass balances to estimate recharge rates or N losses in agricultural regions.

[19] Model simulations indicated a wide range of zero-order O_2 reduction rates ($k_O = 0.0$–1.2 mg L^{-1} yr^{-1}) in the saturated zone. Low k_O values (≤ 0.15 mg L^{-1} yr^{-1}) were obtained for WI, NY, MD/K, MD/L, NE/W, and TX. The persistence of O_2 limited the production of excess N_2 to undetectable levels throughout most of the analyzed portions of these aquifers. At sites with measurable excess N_2 production by denitrification, zero-order denitrification rates

[1]Auxiliary materials are available in the HTML. doi:10.1029/2011WR011008.

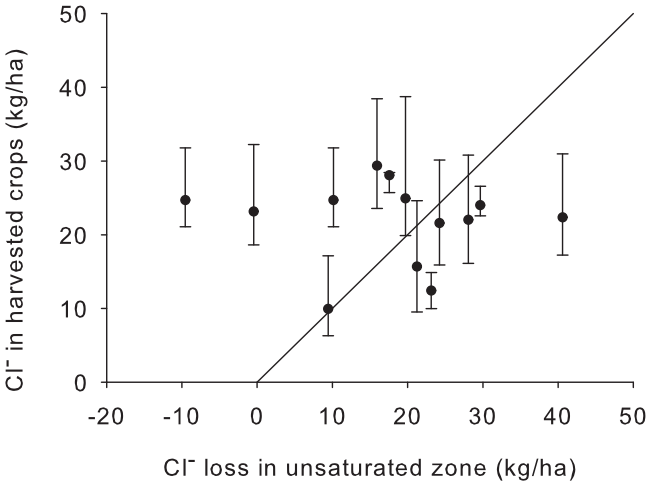

Figure 4. Comparison of estimated apparent Cl^- losses in modeled profiles with independently estimated potential Cl^- losses in harvested crops (Table S3). Error bars represent high and low estimates of Cl^- in harvested crops (Table S2). The diagonal line is 1:1.

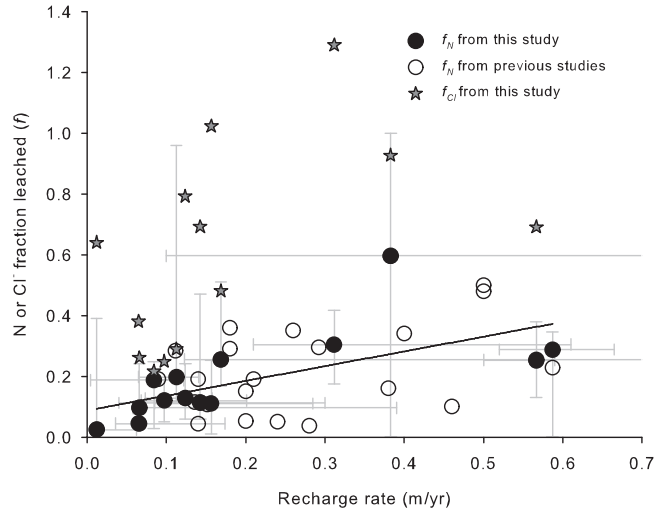

Figure 5. Relation between estimated N or Cl^- leaching fraction, f, and recharge rate, R. Solid symbols represent f_N estimated from the vertical model in this study and open symbols represent f_N estimates from previous studies [*Tesoriero et al.*, 2007; *Puckett et al.*, 2011]. The solid line is a linear regression fit to 14 of the f_N estimates from this study and 15 sites from previous studies. Error bars are nonlinear simultaneous 95% confidence intervals.

ranged from 0.01 to 1.93 mg-N L^{-1} yr^{-1}. The range in calculated denitrification rates is consistent with rates calculated previously at these and other sites using the N_2 gradient method with groundwater dating on decadal timescales [*Green et al.*, 2008b]. Threshold concentrations of O_2 inhibiting denitrification (O_{2cut}) ranged from 0.6 mg L^{-1} to >8 mg L^{-1}. Variability in this parameter might be related to suboxic denitrification; however, previous studies generally do not indicate such a large range of O_{2cut} in groundwater. It is likely that the high values are caused by some combination of the following: heterogeneity within the aquifer or along the well screen can produce mixed samples representing multiple redox conditions [e.g., *Green et al.*, 2010], and combining multiple profiles with varying recharge rates could create the appearance of overlapping redox processes. The model uses a zero-order reaction expression for denitrification and oxygen reduction. To assess whether a concentration-dependent rate might have been appropriate, we checked for a correlation between k_N and N application rate or NO_3^- concentration at the water table and found no correlation. These results indicate that other factors than N concentration such as solid-phase electron donors are likely more important for controlling k_N.

4.2. Relation Between Recharge Rate and Leaching Fractions for N and Cl^-

[20] The relative amounts of N and Cl^- applied to the land surface that ultimately enter groundwater can be affected by different processes in the unsaturated zone. Figure 5 shows the relation between recharge and the fractions of N and Cl^- inputs that reached the water table. Figure 5 indicates that the fraction of N leached is correlated with recharge values ($p = 0.004$) in the range of 0–0.6 m yr^{-1} among the 14 sites in this study and 15 sites from previous studies [*Tesoriero et al.*, 2007; *Puckett et al.*, 2011]. The leaching fraction of N is also correlated with water use efficiency (E), defined as $E = R/(I + P)$, where I is the irrigation rate and P is the annual precipitation rate. Sites where evapotranspiration is relatively large have lower values of f_N (see an additional discussion in section 4.3). Previous unsaturated zone studies provide examples of increased NO_3^- fluxes with increased percolation at individual sites [*Nakamura et al.*, 2004; *Nolan et al.*, 2010], while the current results indicate this relation may apply among multiple sites with diverse geography. The observed relation indicates that the physical factor of water recharge interacted with chemical factors that contribute to N leaching to groundwater. With more recharge, more N apparently is transported below the root zone, resulting in higher N leaching fractions and relatively constant NO_3^- concentrations in shallow groundwater among the study sites. Higher recharge rates may lower residence times in the soil/root zone, resulting in less time for plant uptake or cycling by soil bacteria. Based on previous studies, we expect there was limited influence of mineralization, nitrification, or denitrification on the fate of N between the root zone and water table [*Green et al.*, 2008a]. Clearly, models of agricultural effects on groundwater quality must account for variability of local hydrological and chemical factors affecting the transmission of NO_3^- from soils to aquifers.

[21] The correlation between R and f_N appears to be robust. Based on tests of model uniqueness, estimates of parameter uncertainty, and inference from comparisons with other tracers, the correlation does not appear to result from parameter interdependence in the model calibration. Following the method of *Hill and Tiedeman* [2007], we tested the uniqueness of the calibration and the parameter estimates by recalibrating with varying initial values of the parameters of interest. For all sites, the final parameter values were found to be unique, as shown by the convergence of

each inverse model to the same parameter values regardless of the initial estimates. Moreover, nonlinear simultaneous confidence intervals [see *Hill and Tiedeman*, 2007; *Welch et al.*, 2011] were calculated for R and f_N at all sites to quantify parameter uncertainty (Figure 5). Parameters were not highly correlated, as indicated by the finite confidence intervals. Moreover, the same equations were used to predict both f_{Cl} and f_N, but the values of f_{Cl} did not correlate with recharge rates (see below), which further indicates that the correlation between R and f_N does not stem from parameter interdependence in the model calibration.

[22] Values of f_{Cl} do not appear to be correlated with recharge rates (Figure 5). This is expected because Cl^- neither leaches from, nor is absorbed by, the sediment or soil particles in large quantities in the unsaturated zone. Except in arid environments, Cl^- generally does not accumulate substantially in the unsaturated zone. The Cl^- removed in harvested plants also might not be strongly related to recharge, although Cl^- bioaccumulation could be affected by varying transpiration fluxes or soil water Cl^- concentrations.

4.3. Effects of Evapotranspiration and Soil Type on Leaching Fractions and Concentrations

[23] Evaporatranspiration (ET) and soil type are other factors to consider in the relation between leaching fractions and physical variables. For a given water input and mass flux of a conservative solute, greater fractional loss of water to ET results in higher concentrations (but no change in total mass) of conservative solutes in recharge. Because most agricultural sites have roughly similar inputs of water to meet plant requirements (Table 1), larger losses of water to ET generally correspond to lower values of recharge. The relation among concentration, fractional water loss to ET, and leaching fraction is shown in Figure 6. The x-axis is the fraction of applied water lost to ET (assuming run-on balances runoff) as defined by ET loss $= (P + I - R)/(P + I)$, where P is annual precipitation, I is annual irrigation, and R is annual recharge. The y-axis is the ratio of the observed concentration of NO_3^- or Cl^- in groundwater (C_{obs}) to the applied concentration at land surface computed using the equation $C_{obs}/C_{app} = f_i/(1 - \text{ET loss})$, where f_i is the leaching fraction for N or Cl^- (Table 2). A single point for each site is derived from the data (Table 1) and fitted parameters (Table 2). For each point, the soil drainage class listed in Table 1 is also indicated.

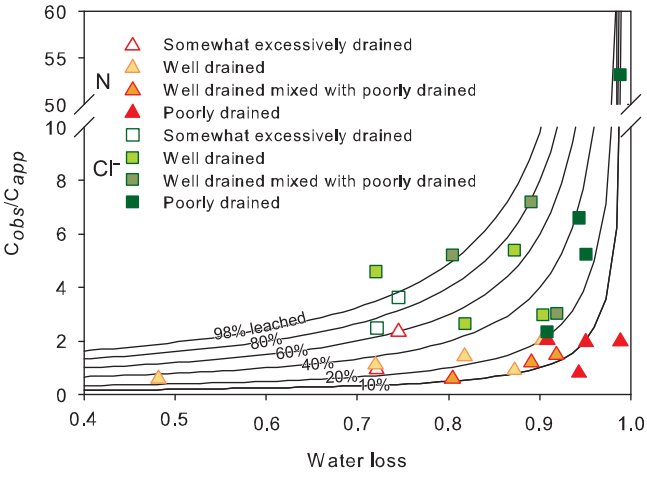

Figure 6. Relation between concentration enrichment and the fraction of applied water lost to evapotranspiration (ET). Concentration enrichment is defined as C_{obs}/C_{app}, where C_{obs} is the observed concentration in groundwater at the water table and C_{app} is the applied concentration based on the total applied load divided by the total water inputs. The curves show the expected increase of C_{obs}/C_{app} with increasing ET for various leaching fractions (mass leached below the root zone/mass applied). Triangles represent NO_3^-; Squares represent Cl^-.

[24] Variations in water losses and soil texture at the studied sites are important factors influencing the leaching fractions of N and Cl^- (Figure 6). For a constant leaching fraction, f_N, each curve shows the expected increase of C_{obs}/C_{app} with increasing water loss. Aquifers with higher values of f_N tended to be overlain by well drained or somewhat excessively drained soils; whereas lower f_N values occurred in aquifers beneath soils with mixtures of well- and poorly drained or poorly drained textures. Based on a Wilcoxon-Mann-Whitney test, the mean f_N value for poorly drained sites was significantly lower than for well drained sites (0.10 and 0.23 respectively, $p = 0.007$).

[25] *Green et al.* [2008a] reported that among five agricultural sites (also included in this study), the sites with sandy soils had relatively high-f_N values, whereas the finer-grained soils had lower-f_N values. In this study, the results of the nine additional sites are consistent with those earlier results. In more-well drained soils, NO_3^- moves more quickly to the water table and there is reduced opportunity for denitrification, plant uptake, or incorporation into organic matter. In contrast, more poorly drained soils with high ET and limited groundwater recharge may promote slower transport and often contain sufficient organic matter to support denitrification in soils under partially or fully saturated conditions. Loss of water and solutes to runoff may also contribute to the trend of lower-f_N values in more poorly drained soils.

[26] The NO_3^- concentration factor in recharge, C_{obs}/C_{app}, varies among sites within a narrow range (0.6–2) compared to that of Cl^- (2–53). The difference in relative concentration ranges relates to the differences in the leaching fraction discussed in section 4.1. The positive correlation of f_N with R corresponds to relatively constant concentrations among sites. In contrast, the more widely varying f_{Cl} corresponds to greater Cl^- concentrations at sites with low recharge and high ET. In addition, concentration factors of NO_3^- appear to be uncorrelated with the soil drainage type (Figure 6). This lack of correlation of NO_3^- concentration factors with soil type has relevance to the findings of a previous national statistical study [*Nolan and Hitt*, 2006] showing that NO_3^- concentrations at depths of ~4–29 m tend to be lower beneath more poorly drained soils. The combined results of the current and previous study indicate that the relation between poor soil drainage and lower NO_3^- concentrations at depth may result from diminished migration of NO_3^- beneath poorly drained soils as a result of lower vertical velocities and interception by

tile drains rather than from lower concentrations leaving the unsaturated zone.

4.4. Vertical Distribution of Reaction Rates

[27] Major uncertainty in assessing aquifer vulnerability stems from limited knowledge of the spatial variability of reaction rates of O_2 and NO_3^-. In these reactions, subsurface microbes can consume electron donors originating in recharging water or from solid-phase aquifer materials such as organic carbon, ferrous iron, and reduced S minerals [*Korom*, 1992; *Rodvang and Simpkins*, 2001]. The distribution and relative importance of these potential reactants is difficult to predict. Mass balance studies commonly indicate relative importance of solid phase electron donors in aquifers over surface-derived dissolved organic carbon [*Postma et al.*, 1991; *Böhlke and Denver*, 1995; *Böhlke et al.*, 2002, 2007b; *Beller et al.*, 2004; *Green et al.*, 2008b]. Estimated zero-order rates of O_2 reduction and denitrification are summarized in Figure 7 and Table 2. The uniqueness of estimates of k_O and k_N was tested using the same method as described in section 4.2. All estimates of k_O and k_N were found to be unique. Nonlinear simultaneous confidence intervals were calculated for k_N and k_O to evaluate relative uncertainty in parameter estimates among sites. Parameter confidence intervals were finite at most sites, but some sites have no upper confidence limit for k_N due to noisy data (IA and NE/W) and insufficient vertical data resolution to determine the upper limit of the rate of denitrification (MN, CA, and NE/E). For some sites, there was no measurable k_N because O_2 inhibited denitrification throughout the sampled portions of the aquifers and excess N_2 remained below detection limits (e.g., 1.3 mg L^{-1} in the work of *Green et al.* [2008b]). In Figure 7, solid symbols represent reaction rate estimates from this study, and open symbols represent estimates from previous studies using age tracers, excess N_2, and O_2 data [*McMahon et al.*, 2004a, 2004b]. To facilitate comparison, reaction rates were converted to electron transfer rates. The electron transfer equivalent for O_2 reduction was four times the molar O_2 reduction rate, and the electron transfer equivalent for denitrification was five times the molar denitrification rate (as N). As shown in Figure 7, sites with high k_N also had high k_O. The 1:1 line represents the trend at which the rate of electron transfer of O_2 reduction is equal to that of denitrification. Most of the estimated rates plotted below the 1:1 line, indicating that the rates of electron transfer for denitrification were higher than for O_2 reduction. Exact ratios are given in Table 2. As shown by equation (2), denitrification in recharging groundwater typically follows O_2 reduction and occurs at or below the depth of O_2 reduction. Therefore, greater rates of electron transfer for denitrification indicate greater rates of electron transfer in deeper portions of the aquifers.

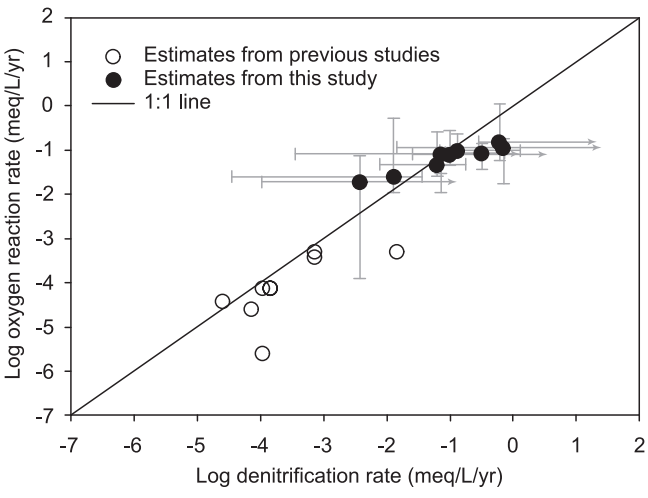

Figure 7. Relation between oxygen reduction rate and denitrification rate in electron milliequivalents (meq L^{-1} yr^{-1}) on log scale. Solid symbols represent estimates from the model in this study and open symbols represent estimates from previous studies [*McMahon et al.*, 2004a, 2004b]. Error bars are nonlinear simultaneous 95% confidence intervals. An arrow head on the end of an error bar indicates no limit was obtained (5 sites).

[28] The vertical differences in electron transfer rates indicate biogeochemical factors vary with depth. Microbial populations in the shallow saturated zone are commonly reported to be uncorrelated with depth [e.g., *Ayuso et al.*, 2009]. Differences in kinetics of O_2 or NO_3^- reactions with a particular substrate are unlikely to explain the more rapid electron transfer in some NO_3^- reducing zones in this study. The greater reduction potential of O_2 typically creates a greater tendency for aerobic reactions, rather than anaerobic reactions, to occur [*Fuhrmann*, 1998]. Most likely, the reactivity of solid-phase electron donors changes with depth, with more labile donors being depleted in shallow sediments from prolonged exposure to oxidizing waters, leading to the observed pattern of higher-electron transfer rates at depth in most of the aquifers. Previous studies at many of the sites summarized in Figure 7 indicated that dissolved electron donors from recharging water were insufficient to account for losses of O_2 and NO_3^- at the aquifer scale, and relict, solid-phase materials in the aquifer were likely the primary sources of electron donors for O_2 reduction and denitrification [*Böhlke and Denver*, 1995; *Böhlke et al.*, 2002; *Green et al.* 2008b]. At the MN site, for example, *Böhlke et al.* [2002] concluded that the position of the denitrification zone could be explained by consumption of reactive Fe-sulfide minerals in the upper part of the aquifer by oxic recharge water over a period of $\sim 10^4$ yr since the glacial outwash aquifer was established.

[29] Three sites in this study (NE/W, WA, and CA) and one site from a previous study had greater estimated O_2 reduction rates than denitrification rates. This behavior could result from a supply of dissolved organic carbon from the surface, or it may be a result of uncertainties in the estimated reaction rates. To test the possibility that higher-manure applications were associated with higher DOC at some sites, we checked for a correlation between the denitrification rate or O_2 reduction rate and the percentage of manure in total N applied in the last 10 yr (2%–49%), and found no significant relationship. Uncertainty in the estimated parameters is a feasible explanation. These sites had relatively noisy concentration profiles combined with very low concentrations of excess N_2 near detection limits, which led to relatively large confidence intervals on parameter estimates (Figure 7). The prevalence of sites with higher-electron transfer rates for denitrification than for shallow oxygen reduction suggests that: surface derived

DOC is not a major electron donor source at most of these sites; solid phase electron donors dominate denitrification reactions; solid phase electron donors also dominate O_2 reactions; and microbially mediated electron transfer rates can increase with depth (at least down to the depths considered in this study) as a result of weathering front migration.

[30] Our results indicate the relation between electron donors and denitrification rate is an important topic for future study [see also *Böhlke and Denver*, 1995; *Robertson et al.*, 1996; *Rodvang and Simpkins*, 2001; *Böhlke et al.*, 2002; *McMahon and Chapelle*, 2008]. In this study, DOC and solid-phase electron donor concentrations were not available at all sites. Improving understanding of the sustainability of denitrification will require additional information about the reactivity and abundance of the heterogeneously distributed reductants in aquifers.

4.5. Assessment of Calibrated Models

[31] Section 4.5 describes the current model's comparability with previous studies, sources of uncertainty, and applicability to other areas with more limited data. As discussed previously, the vertical transport model is designed for agricultural areas where mass input at the land surface is spatially uniform. The model assumes the flow system is in the recharge area so sample locations must be chosen from recharge areas at all sites. Samples taken from areas of low topography or near gaining surface water bodies must be excluded to avoid areas affected by upward groundwater fluxes.

[32] Care must be taken in comparing current results to previous site-specific studies. The uniformly applied modeling approach at sites with multiple profiles yields calibrated parameters that represent spatial averages and can be subject to stronger scaling effects than detailed local estimates from site-specific studies. The regionally averaged parameters should not necessarily supersede results reported in the site-specific literature. Furthermore, whereas some previous studies at these sites derived recharge fluxes and reaction rates directly from interpretations of apparent groundwater age, our calculations are based on depth profiles and a vertical age distribution model following the conceptual model in Figure 2. Where age interpretations are difficult or where additional tracers like Cl^- help to constrain vertical velocities, our approach using selected vertical profiles in recharge areas and calibrating directly against tracer concentrations may reduce the uncertainty of hydrologic and geochemical parameters. Alternatively, where groundwater ages are well characterized and processes are related to time, but recharge rates and flow paths are not spatially uniform, our approach may increase uncertainties of estimated parameters. For future work, hydrologic variability can be incorporated into the vertical flux model, for example, by applying multiple recharge rates and a single set of reaction parameters. Exploratory analysis at the CA site indicated that this approach reduced the model error and parameter uncertainty (results not shown).

[33] There are multiple sources of uncertainties in the model inputs including the scale of the study and estimates of application rates. Of the 14 study sites, 10 had samples collected from multiple locations. For some sites with large study areas, including IA, WA, NE/W, multiple sample locations (more than three) were combined to form one profile. These sites had scattered NO_3^-, Cl^-, and excess-N_2 data, which may result from nonuniform water input or fertilizer applications, or from varying aquifer thickness. These variations due to multiple locations and large study areas contributed to uncertainty of the parameters for these three sites. Although the multiple profiles of NO_3^-, Cl, and excess-N_2 were noisy in the IA and WA sites, age tracer, and O_2 profiles were less scattered, such that combining profiles resulted in less uncertainty in the model calibration. Other sites for which combining multiple locations better constrained the model calibration were MD/K, MD/L, CA, NE/E, NC, NY, and TX. At these sites, the multiple profiles were similar for each individual solute and the combined vertical profiles were comparable to the temporal variations in applied chemicals and age tracers. The MS, MN, MD/A, and WI sites had only one sampling location and the historical application rates provided good matches with the concentration profiles at these sites. As discussed above, multiple sampling locations can improve the model calibration and the prediction but estimated parameters represent averages of the conditions among lumped profiles and may differ from local estimates.

[34] As mentioned previously, county-level estimates of N and Cl^- inputs can over- or underestimate the local conditions. However, for most of the sites considered in this study, the shapes of the NO_3^- and Cl^- concentration profiles in groundwater corresponded well with the historic application rates.

[35] Although most of the sites used in this study had relatively rich data sets of dissolved gases and age tracers, the model can be applicable for sites with smaller datasets that may not include dissolved gases or age tracers. The model was applied to predict the fate and transport of nitrate in shallow groundwater in northwestern Mississippi without calibration to age-tracers [*Welch et al.*, 2011] and yielded recharge estimates within the range of several previous studies. In that case the excess N_2 constrained the denitrification rate and the shape of the Cl^- profile correlated with the historical application data. At sites with large vertical gradients in NO_3^- and Cl^-, and aerobic groundwater such as MD/L and WI, excess N_2 is not needed and the historical application rate can be used to fit the vertical groundwater profiles.

5. Future Projections of Nitrate Profiles

[36] Depending on groundwater denitrification rates, NO_3^- concentrations in recharge can potentially advance unabated into deeper portions of the aquifer. The most recently measured distribution of NO_3^- may not give an accurate view of the long-term vulnerability under recent land use and hydrology. In section 5 we present the results of projections of the NO_3^- model profiles into the future when the vertical concentration profiles no longer change with time and thus reach steady state. These projections were used to identify the relative importance of N inputs, biogeochemical processes, and physical aquifer properties in forecasts of NO_3^- contamination in groundwater and to evaluate the vulnerability of the aquifers. To create these projections the applied masses were held constant at the 2001 values at each site. Vulnerability was characterized using two measures of NO_3^- distribution in the steady state profiles: depth of NO_3^- extinction (Z_{ss}), and total mass of

NO_3^- in the aquifer (T_{ss}). The depth of NO_3^- extinction (Z_{ss}) is defined as the depth beneath the water table where the steady state NO_3^- concentration profile reaches zero. From equations (1)–(5), the analytical solution for Z_{ss} is:

$$Z_1 = H_s\left[1 - \frac{1}{\exp\left(\frac{(C_{O_0} - C_{O_{cut}})R}{n_s H_s k_O}\right)}\right], \tag{7}$$

$$Z_{ss} = H_s\left[1 - \frac{1}{\exp\left(\frac{M_N f_N + (C_{O_0} - C_{O_{cut}})k_N R/k_O}{n_s H_s k_N}\right)}\right], \tag{8}$$

where Z_1 is the depth below the water table of the zone with O_2 reduction without denitrification and ($Z_{ss} - Z_1$) is the thickness of the denitrification zone. For estimates of total mass in the aquifer, the concentration of NO_3^- within the denitrification zone was approximated by a linear decrease with depth. The analytical solution for NO_3^- mass storage in groundwater, T_{ss} (M L^{-2}) in the steady state profiles is equal to the sum of NO_3^- mass in the aerobic zone (T_{ss1}) and in the denitrification zone (T_{ss2}) given by the equations:

$$T_{ss1} = n_s\left(\frac{M_N f_N}{R}\right)Z_1 \tag{9}$$

and

$$T_{ss2} = \frac{n_s}{2}\left(\frac{M_N f_N}{R}\right)(Z_{ss} - Z_1), \tag{10}$$

where all variables are defined as before. Based on the correlations between f_N and R (Figure 5) and between k_O and k_N (Figure 7) these pairs of parameters were varied proportionally for each site by substituting $R \times f_{N\mathrm{cal}}/R_{\mathrm{cal}}$ for f_N and $k_N \times k_{O\mathrm{cal}}/k_{N\mathrm{cal}}$ for k_O in equations (7)–(10), where the subscript "cal" indicates the calibrated value of the parameter for that site. For sites with aerobic conditions in the sampled zone (as described in section 4.4), k_N below the sampling zone was inferred from k_O using a best-fit line through the estimated values of k_N and k_O for all sites with observed denitrification. All values of k_N inferred from k_O were low, ranging from 0 to 0.015 mg-N L^{-1} yr^{-1}.

[37] To investigate the susceptibility to continuing NO_3^- contamination of the 14 studied aquifers, the most recent depth of NO_3^- extinction (Z_{curr}) was compared to that at steady state (Z_{ss}) (Figure 8). For purposes of comparison, Z_{curr} was based on the time of the field study at each site (Table S1) and set equal to the smaller of the depth at which the modeled NO_3^- concentration reaches zero or the depth at which the date of application, $t' = 1945$ (assumed to be the starting date for mass production of chemical fertilizers). Case (2) was applied at sites such as TX with background NO_3^- in premodern water from unknown sources. The value of Z_{ss} for each site at steady state is from equation (8) using calibrated parameter values (Table 2). In Figure 8, the values of NO_3^- extinction depth Z_{curr} and Z_{ss} are divided by the thickness of each aquifer, H_s, to give values between 0 and 1, where a value of 0 occurs at the water table and a value of 1 is at the bottom of the aquifer. For the purposes of discussion in the remainder of the paper,

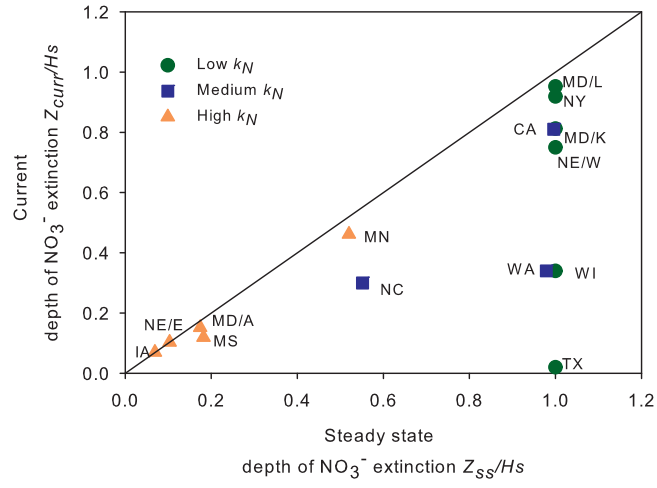

Figure 8. Comparison of depth of NO_3^- extinction for recent (Z_{curr}) and steady state (Z_{ss}) conditions at each site normalized by the aquifer thickness (H_s). Depth of NO_3^- extinction at steady state is from equation (8), using constant N mass applications after 2001. Circles are sites with low k_N (<0.05 mg-N L^{-1} yr^{-1}), squares are sites with medium k_N (0.05–0.25 mg-N L^{-1} yr^{-1}), and triangles are sites with high k_N (>0.25 mg-N L^{-1} yr^{-1}).

aquifers with estimated or inferred denitrification less than 0.05 mg-N L^{-1} yr^{-1} are called "low k_N," including TX, NE/W, MD/K, MD/L, WI, and NY; aquifers with medium rates are called "medium k_N,"(k_N ranging from 0.05 to 0.25 mg-N L^{-1} yr^{-1}), including CA, WA, and NC; and the remaining sites are called "high k_N"($k_N > 0.25$ mg-N L^{-1} yr^{-1}), including MD/A, NE/E, MS, MN, and IA.

[38] Aquifers with values of Z/H_s on the 1:1 line in Figure 8 were near steady state at the study date and those under the 1:1 line had not reached steady state. Table 2 lists the time required for each aquifer to reach steady state. All five of the high-k_N aquifers were near steady state. In high-k_N aquifers, denitrification quickly removes N from groundwater (after O_2 is reduced) and can maintain a near steady state profile. At such sites, the total depth of the NO_3^- profiles may remain close to the most recent depth, although eventually the depth will increase as solid-phase electron donors are depleted. Most aquifers with low-k_N and medium-k_N values were not at steady state. The TX, WA and WI sites were not close to steady state because of their combination of lower k_N and greater aquifer thickness (100, 100, and 50 m for WA, TX, and WI, respectively). At the time of sampling, NO_3^- contamination from modern agricultural practice had only reached the shallower portion of these aquifers. Because of low k_N values, the NO_3^- fronts were predicted to continue migrating deeper until extinction depths at steady state approach the bottoms of these aquifers. As discussed in section 4.5, parameters and assumptions for the analytical steady state profiles may not apply locally at sites with spatially variable hydrology such as focused recharge beneath leaky canals (NE/W) [*Böhlke et al.*, 2007b] or playas (TX) [*Fryar et al.*, 2000]. At these heterogeneous sites with multiple profiles, point- or line-sources of recharge may create noise in the vertical profiles with corresponding

uncertainty in local predictions. However, the parameters appeared to be representative of average regional conditions.

5.1. Sensitivity of Steady State NO_3^- Mass and Depth to Physical and Chemical Factors

[39] To compare the relative importance of different parameters to the predicted depth of NO_3^- extinction, Z_{ss}, and NO_3^- total mass storage in groundwater, T_{ss}, a sensitivity parameter (S_y) was calculated with respect to parameters M_N, R, f_N, k_N, and k_O. Parameters that more strongly affect Z_{ss} or T_{ss} have larger absolute values of S_y. The sensitivities, S_y, were calculated as

$$S_y = \frac{\partial y}{\partial b}|b|, \tag{11}$$

where y is a prediction, such as Z_{ss} or T_{ss}; b is a calibrated parameter such as M_N, R, f_N, k_N, or k_O; and $\partial y/\partial b$ is the derivative of Z_{ss} or T_{ss} with respect to the parameter, calculated from equations (7)–(10). These sensitivities reflect the linear change in the predicted value of Z_{ss} (m) or T_{ss} (g m^{-2}) in relation to a fractional change of a parameter (unitless). For example, at the MN site R was 0.10 m yr^{-1}, $\partial Z_{ss}/\partial R$ was 40.3 m yr m^{-1} and S_y was 4.0 m. In other words, a 100% increase of R to 0.20 m yr^{-1} corresponded to a 4.0 m increase of Z_{ss}, a 200% increase of R to 0.30 m yr^{-1} corresponded to a 8.0 m increase of Z_{ss}, and so on. As a parameter increases, positive values of S_y indicate the prediction, y, increases, while negative values indicate the prediction decreases. Sensitivities were evaluated at the calibrated parameter values. Calculated sensitivities of Z_{ss} (S_Z) and T_{ss} (S_T) to changes in the parameters are presented in Table S4 and the absolute values of these sensitivities are plotted in Figure 9 to illustrate their relative importance.

[40] The sensitivities of Z_{ss} (S_Z) varied among sites (Figure 9A). For low-k_N aquifers, S_Z was <0.05 m, which implies that none of parameters (R, f_N, M_N, k_O, and k_N) have a strong influence on the steady state depth of NO_3^- extinction, as a result of conservative migration of NO_3^- to near the bottom of the aquifer. Because vertical velocities approach zero and isochrons are close together toward the bottom of the aquifers (see equation (5)), changes in the time of persistence of NO_3^- had a relatively small effect on the displacement of Z_{ss} near this boundary. For high-k_N aquifers, the extinction depths were also relatively insensitive, but for a different reason. In these aquifers the extinction depths were small. Even though doubling the applied mass approximately doubled the thickness of the zone of denitrification, there was still small change in Z_{ss}, and hence small sensitivity. For medium-k_N aquifers, the extinction depths were larger but were not close to the bottom of the aquifer. Therefore, changes in parameters controlling NO_3^- flux change the depth of NO_3^- extinction substantially.

[41] Figure 9B illustrates the sensitivity of T_{ss} (S_T), which varied among sites. The high-k_N aquifers had S_T lower than 30 g m^{-2} over the range of parameter variations. At these sites fractional changes in the parameters had a more limited effect on T_{ss} because the NO_3^- leaching to the water table was quickly eliminated by denitrification and so the total mass of NO_3^- in the aquifer was relatively small. Doubling of the depth and mass of NO_3^- resulted in small

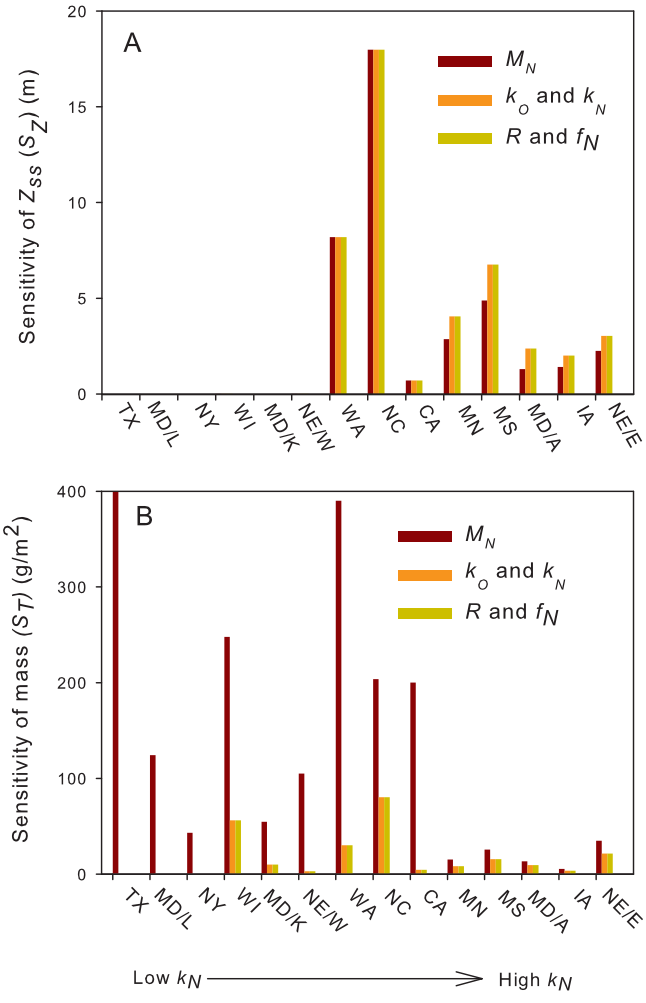

Figure 9. Sensitivities (S_y) for depth of (a) NO_3^- extinction (Z_{ss}) and (b) NO_3^- − N mass storage in groundwater (T_{ss}) with respect to parameters of mass applied on land surface (M_N), recharge rate (R), denitrification rate (k_N), oxygen reduction rate (k_O), and N leaching fraction (f_N). Sites are ordered by k_N from low to high.

total changes in mass and, therefore, small sensitivities. In contrast, for the remaining aquifers with denitrification lower than 0.25 mg-N L^{-1} yr^{-1} (low-k_N and medium-k_N aquifers), S_T values for mass applied at land surface (M_N) were significantly higher than 30 g m^{-2} and exceeded S_T for other parameters. For these aquifers, changes in the mass applied on land surface could cause substantial long-term changes of N mass storage in groundwater as a result of large NO_3^- storage capacity and limited reactions.

5.2. Nonlinear Changes in Depth of NO_3^- Extinction and Mass Storage in Groundwater

[42] Section 5.1 identified important factors controlling N contamination in groundwater. Section 5.2 further explores the conditions under which these parameters have significant nonlinear effects on aquifer vulnerability. Scenarios included ranges of parameters as proxies for possible future changes in agricultural practices. Figure 10 shows (1) the steady state depth of extinction of NO_3^- for each aquifer based on calibrated parameter values (solid symbols),

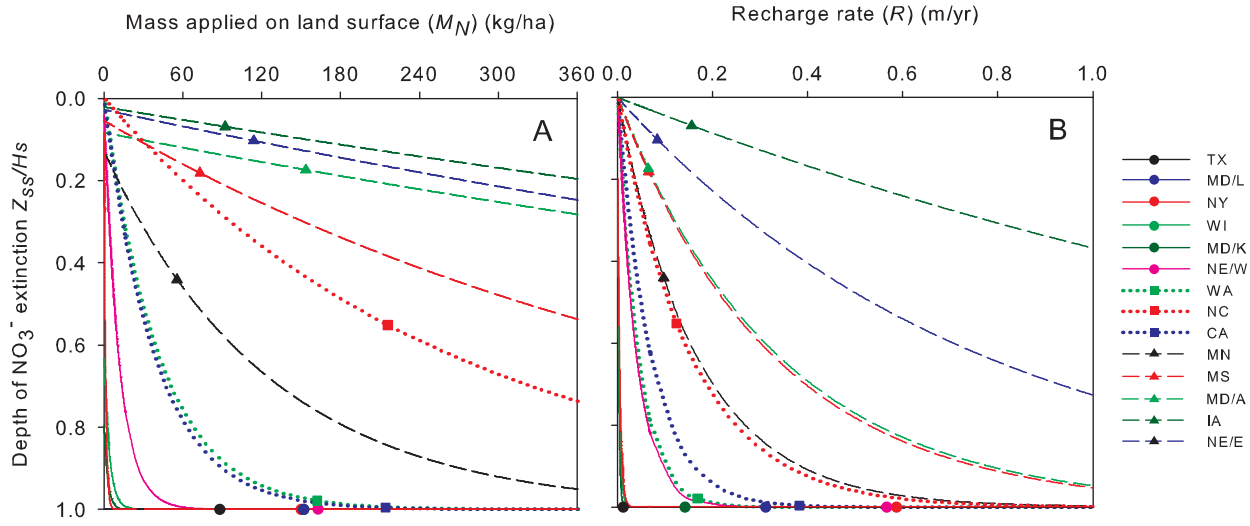

Figure 10. Relationships between the depth of NO_3^- extinction divided by aquifer thickness (Z_{ss}/H_s) and hydrogeological parameters (A) mass applied on land surface (M_N) and (B) recharge rate (R). The symbols are the steady state depth of extinction of NO_3^- for each aquifer based on calibrated parameter values. Circles and solid lines are sites with low k_N (<0.05 mg-N L^{-1} yr^{-1}), squares and dotted lines are sites with medium k_N (0.05–0.25 mg-N L^{-1} yr^{-1}), and triangles and dashed lines are sites with high k_N (>0.25 mg-N L^{-1} yr^{-1}). Curves are from analytical solutions at steady state (equations (7) and (8)). Nitrogen mass applied at land surface remains constant after 2001 for the steady state calculation (Table 1). On the y-axis, 0 corresponds to the water table and 1 corresponds to the bottom of the aquifer.

and (2) curves determined by varying either M_N (Figure 10A) or R (Figure 10B) while holding all others constant.

[43] Figure 10A shows the effects of varying N inputs on the projected NO_3^- extinction depths, Z_{ss}, in the 14 aquifers. The concentration of NO_3^- in shallow aquifers has been observed to correlate spatially with gross differences in N applications at the land surface [*Nolan et al.*, 2002; *Nolan and Hitt*, 2006]; however, the relation between Z_{ss} and the mass of N applied on land surface was more complex. Figure 10A illustrates that higher application rates of N result in greater Z_{ss}, as expected. However, sites responded differently to changes in application rates. The aquifers showed two distinct responses for the range of M_N considered here (0–360 kg ha^{-1}): NO_3^- migrated to the bottom of the aquifer ($Z_{ss}/H_s \approx 1$ for all M_N), and NO_3^- never migrated to more than 80% of the total depth of the aquifer ($Z_{ss}/H_s < 0.8$ for all M_N). The first group included low-k_N sites, medium-k_N sites with relatively high recharge rates (CA and WA), and a high-k_N site with moderate recharge and small aquifer thickness (MN) (Table 2). For aquifers in this group, the depth of NO_3^- extinction changed most rapidly (S_Z was greatest) at low values of M_N (0–80 kg Ha^{-1} yr^{-1}) (Figure 10A). The second group included the remaining high-k_N sites and a medium-k_N site with a relatively low recharge rate (NC). At high denitrification and low recharge rates, denitrification attenuated NO_3^- in shallow groundwater and prevented the NO_3^- from reaching deeper groundwater, even at higher rates of N application.

[44] Recharge strongly affects the eventual depth of extinction of NO_3^- as shown in Figure 10B. For 12 of the aquifers, increasing the recharge rate up to 1 m yr^{-1} resulted in NO_3^- migration to more than 80% of the total depth (Figure 10B). Generally, the depth of NO_3^- extinction changed most rapidly when the recharge rates were lower than 0.15 m yr^{-1}. The curves leveled off when the NO_3^- front approached the bottom of the aquifer (Z_{ss}/H_s greater than ~0.6). Approximately half of the 14 modeled aquifers had estimated recharge rates higher than 0.15 m yr^{-1} and the steady state depths of NO_3^- extinction in those aquifers were >80% of the aquifer thicknesses. Optimizing water use and infiltration in agricultural areas therefore plays a vital role as a best management practice (BMP) affecting groundwater quality. The recharge rate has changed greatly as a result of irrigation in areas such as the Central Valley, CA [*Burow et al.*, 2010] and the High Plains [*McMahon et al.*, 2007]. In irrigated settings efforts to decrease application of excess water may have an additional benefit of decreasing transport of N to groundwater. It is well known that tile drains below agricultural lands can rapidly transport applied N to surface water [*Crumpton et al.*, 2006] and efforts to address this problem have been proposed. In addition there has been much effort to control nitrogen loading to streams, lakes, estuaries and other surface water by increasing recharge with retention basins, and increasing or preserving permeable surfaces in watersheds. Our study results indicate that the compound water quality effects of recharge on vertical velocity and leaching fraction should be considered in any efforts to manage runoff of N to surface water by increasing infiltration, as this practice may transfer the nitrate problem from a surface water issue to a groundwater issue.

[45] While the depth of NO_3^- extinction gives information about the extent of contamination and likelihood of deep groundwater being affected, total mass storage in groundwater, T_{ss}, depends on depth and concentration. Mass storage depends on both the distribution and concentration of NO_3^-. Similar to results for N extinction depth, T_{ss} responded nonlinearly to mass of N applied at the

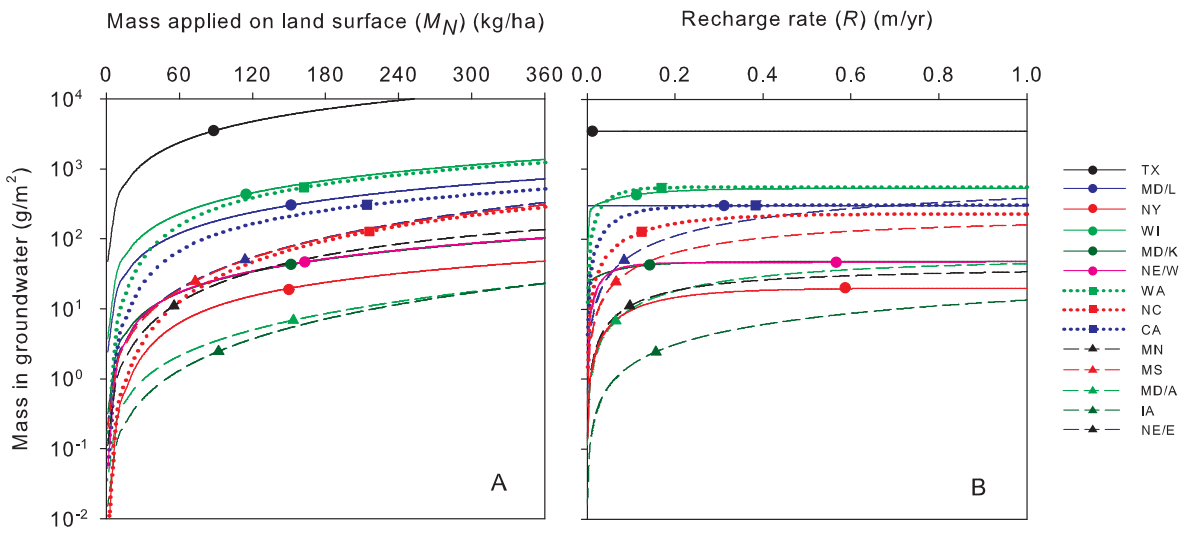

Figure 11. Relation between steady state mass storage (log scale) in groundwater and hydrogeological parameters (A) mass applied on land surface (M_N) and (B) recharge rate (R). The symbols are the steady state mass in groundwater for each aquifer based on calibrated parameter values. Circles are sites with low k_N (<0.05 mg-N L^{-1} yr^{-1}), squares are sites with medium k_N (0.05–0.25 mg-N L^{-1} yr^{-1}), and triangles are sites with high k_N (>0.25 mg-N L^{-1} yr^{-1}). Curves are from analytical solutions (equations (9) and (10)), with variation of the parameter of interest while all other parameters remain unchanged at calibrated values.

surface (Figure 11A) and recharge (Figure 11B). At steady state, NO_3^- storage in groundwater, T_{ss}, increased with increasing recharge rates and changed substantially when the recharge rates were less than 0.15 m yr^{-1} (Figure 11B). The more pronounced effects at low R were a result of limited storage space in the aquifers. As R increased, the NO_3^- extinction depth, Z_{ss}, also increased and created a greater storage volume of NO_3^-. At higher values of R, however, the effects of increasing R on T_{ss} diminished because Z_{ss} asymptotically approached $Z_{ss}/H_s = 1$, and NO_3^- storage space approached a constant value. For nine out of 14 studied sites, the recharge rates were lower than 0.15 m yr^{-1} and a small change of recharge from the current value can result in a large change of potential N mass storage in groundwater. Shifts in agricultural practices may change the recharge rate through changes in irrigation or crop water use and, therefore, could cause changes in N mass storage in groundwater.

6. Summary

[46] A simple vertical transport model was used to simulate NO_3^- and Cl^- fluxes in groundwater at 14 agricultural sites in different hydrogeological settings. Calibrated parameters including recharge rate, N leaching fraction, O_2 reduction rate, and denitrification rate in the saturated zone were used to characterize the vulnerability of the aquifers under constant loadings equal to modern values. The model results illustrate the relations among physical and chemical factors that control N storage and fluxes in groundwater and provide insight into the most important factors.

[47] The N leaching fraction was positively correlated with recharge rate among the 14 sites. Also, N leaching fractions were correlated with soil drainage class and water loss. Aquifers with higher-leaching fractions of N tended to have well drained or somewhat excessively drained soils. Geochemical factors of denitrification rate and O_2 reduction rate were positively correlated and denitrification rates in a number of cases were higher than O_2 reduction rates on a molar electron basis. Comparison of these rates indicated that solid phases in aquifers were the dominant electron donor sources for these two reactions and electron transfer rates may be slower in the shallower O_2 reduction zone than in the deeper denitrification zone.

[48] Vertical NO_3^- fluxes below the water table historically were affected by a combination of geochemical factors, physical factors, and land use. Models indicated about half of the aquifers were at or near steady state in terms of the total depth of NO_3^- contamination. For scenarios in which 2001 N loading rates were applied in the future, continued downward migration of NO_3^- fronts was predicted at most sites with denitrification rates below 0.25 mg-N L^{-1} yr^{-1}. The steady state depth of NO_3^- depended to a similar degree on application rate, leaching fraction, recharge, and NO_3^- and O_2 reaction rates. Steady state total mass in the aquifer depended primarily on the N application rate. The results from the sensitivity analysis highlight the relative importance of controlling mass application rates over aquifers with low denitrification rates. Aquifers with denitrification rates higher than 0.25 mg-N L^{-1} yr^{-1} are protected from deeper (e.g., >20–30 m) NO_3^- contamination as long as recharge rates are not excessively high, and the supplies of solid-phase electron donors are not depleted, although increases of shallow concentrations and lateral transport of NO_3^- may still be a concern.

[49] **Acknowledgments.** This study was conducted as part of National Research Program and the USGS National Water Quality Assessment Program. Ronald J. Baker, Richard L. Smith and three anonymous reviewers provided helpful suggestions for the manuscript.

References

110th United States Congress (2007), Energy Independence and Security Act of 2007.

Alexander, R. B., and R. A. Smith (1990), County level estimates of nitrogen and phosphorus fertilizer use in the United States, 1945 to 1985, *U.S. Geol. Surv. Sci. Invest. Rep. 90-130*, 12 pp., Reston, Virginia.

Ayuso, S. V., M. C. Guerrero, C. Montes, and A. I. Lopez-Archilla (2009), Spatiotemporal distribution of microbial communities in a coastal, sandy aquifer system (Donana, SW Spain), *Geobiology*, *7*(1), 66–81.

Beller, H. R., V. Madrid, G. B. Hudson, W. W. McNab, and T. Carlsen (2004), Biogeochemistry and natural attenuation of nitrate in groundwater at an explosives test facility, *Appl. Geochem.*, *19*, 1483–1494.

Böhlke, J. K. (2002), Groundwater recharge and agricultural contamination, *Hydrogeol. J.*, *10*(1), 153–179.

Böhlke, J. K., and J. M. Denver (1995), Combined use of groundwater dating, chemical, and isotopic analyses to resolve the history and fate of nitrate contamination in two agricultural watersheds, Atlantic Coastal-Plain, Maryland, *Water Resour. Res.*, *31*(9), 2319–2339.

Böhlke, J. K., R. Wanty, M. Tuttle, G. Delin, and M. Landon (2002), Denitrification in the recharge area and discharge area of a transient agricultural nitrate plume in a glacial outwash sand aquifer, Minnesota, *Water Resour. Res.*, *38*(7), 1105, doi:10.1029/2001WR000663.

Böhlke, J. K., M. E. O'Connell, and K. L. Prestegaard (2007a), Ground water stratification and delivery of nitrate to an incised stream under varying flow conditions, *J. Environ. Qual.*, *36*(3), 664–680.

Böhlke, J. K., I. M. Verstraeten, and T. F. Kraemer (2007b), Effects of surface-water irrigation on sources, fluxes, and residence times of water, nitrate, and uranium in an alluvial aquifer, *Appl. Geochem.*, *22*(1), 152–174.

Böhlke, J. K., P. B. Hatzinger, N. C. Sturchio, B. H. Gu, I. Abbene, and S. J. Mroczkowski (2009), Atacama perchlorate as an agricultural contaminant in groundwater: Isotopic and chronologic evidence from Long Island, New York, *Environ. Sci. Technol.*, *43*(15), 5619–5625.

Burow, K. R., B. T. Nolan, M. G. Rupert, and N. M. Dubrovsky (2010), Nitrate in groundwater of the United States, 1991–2003, *Environ. Sci. Technol.*, *44*(13), 4988–4997, doi:10.1021/es100546y.

Burt, T. P., A. L. Heathwaite, and S. T. Trudgill (Eds.) (1993), *Nitrate: Processes, Patterns, and Management*, 444 pp., John Wiley, N.Y.

Busenberg, E., and L. N. Plummer (1992), use of chlorofluorocarbons (CCL3F and CCL2F2) as hydrologic tracers and age-dating tools—the alluvium and terrace system of central Oklahoma, *Water Resour. Res.*, *28*(9), 2257–2283.

Busenberg, E., and L. N. Plummer (2000), Dating young groundwater with sulfur hexafluoride: Natural and anthropogenic sources of sulfur hexafluoride, *Water Resour. Res.*, *36*(10), 3011–3030.

Cassman K. G., A. Dobermann, and D. T. Walters (2002), Agroecosystems, nitrogen-use efficiency, and nitrogen management, *Ambio*, *31*(2), 132–140.

Crumpton, W. G., G. A. Stenback, B. A. Miller, and M. J. Helmers (2006), Potential benefits of wetland filters for tile drainage systems: Impact on nitrate loads to Mississippi river sub-basins, *Final project report IOW06682*, 34 pp, U.S. Depart. of Agriculture, Ames, Iowa.

Debernardi, L., D. A. De Luca, and M. Lasagna (2008), Correlation between nitrate concentration in groundwater and parameters affecting aquifer intrinsic vulnerability, *Environ. Geol.*, *55*(3), 539–558.

Delin, G. N., R. W. Healy, M. K. Landon, and J. K. Böhlke (2000), Effects of topography and soil properties on recharge at two sites in an agricultural field, *J. Am. Water Resour. Assoc.*, *36*(6), 1401–1416.

Dubrovsky, N. M., et al. (2010), Nutrients in the nation's streams and groundwater, 1992–2004. *U.S. Geol. Surv. Circ. 1350*, 174 pp.

Eckhardt, D. A. V., and P. E. Stackelberg (1995), Relation of groundwater quality to land-use on LongI Island, New York, *Ground Water*, *33*(6), 1019–1033.

Evans, T. A., and D. R. Maidment (1995), A spatial and statistical assessment of the vulnerability of Texas groundwater to nitrate contamination, *Center for Research in Water Resources Online Report 95-2*, The University of Texas at Austin, Austin, TX, available at http://www.crwr.utexas.edu/gis/gishydro00/library/evans/rep95_4.htm.

Frind, E. O., W. H. M. Duynisveld, O. Strebel, and J. Boettcher (1990), Modeling of multicomponent transport with microbial transformation in groundwater: The Fuhrberg case, *Water Resour. Res.*, *26*(8), 1707–1719.

Fryar, A. E., S. A. Macko, W. F. Mullican, K. D. Romanak, and P. C. Bennett (2000), Nitrate reduction during ground-water recharge, southern high plains, Texas, *J. Contam. Hydrol.*, *40*(4), 335–363.

Fuhrmann, J. J. (1998), Microbial metabolism, in *Principles and Applications of Soil Microbiology*, edited by D. M. Sylvia et al., pp. 189–217, Prentice-Hall, Upper Saddle River, N.J.

Green, C. T., L. H. Fisher, and B. A. Bekins (2008a), Nitrogen fluxes through unsaturated zones in five agricultural settings across the United States, *J. Environ. Qual.*, *37*(3), 1073–1085.

Green, C. T., L. J. Puckett, J. K. Böhlke, B. A. Bekins, S. P. Phillips, L. J. Kauffman, J. M. Denver, and H. M. Johnson (2008b), Limited occurrence of denitrification in four shallow aquifers in agricultural areas of the United States, *J. Environ. Qual.*, *37*(3), 994–1009.

Green, C. T., J. K. Böhlke, B. A. Bekins, and S. P. Phillips (2010), Mixing effects on apparent reaction rates and isotope fractionation during denitrification in a heterogeneous aquifer, *Water Resour. Res. 46*, W08525, doi:10.1029/2009WR008903.

Ground Water Monitoring and Assessment Program (2001), Effects of liquid manure storage system on ground water quality—summary report, Minnesota Pollution Control Agency, St. Paul, Minn., available at http://www.pca.state.mn.us/index.php/view-document.html?gid=6336.

Hallberg, G. R. (1986), Overview of agricultural chemicals in ground water, Proceedings of Conference on Agricultural Impacts on Ground Water, Omaha, Nebraska, 63 pp., National Water Well Association, Dublin, Ohio.

Harvey, F. E., and S. S. Sibray (2001), Delineating ground water recharge from leaking irrigation canals using water chemistry and isotopes, *Ground Water*, *39*(3), 408–421.

Hatfield, J. L., and R. F. Follett (Eds.) (2008), *Nitrogen in the Environment: Sources, Problems, and Management*, 2nd ed., 702 pp., Elsevier, Amsterdam, Netherlands.

Healy, R. W. (2010), *Estimating Groundwater Recharge*, 245 pp., Cambridge Univ. Press, Cambridge, U.K.

Herczeg, A. L., and W. M. Edmunds (1999), Inorganic ions as tracers, in *Environmental Tracers in Subsurface Hydrology*, edited by P. G. Cook and A. L. Herczeg, pp. 31–77, Kluwer, Boston, Mass.

Hill, M. C., and C. R. Tiedeman (2007), *Effective Groundwater Model Calibration: With Analysis of Data, Sensitivities, Predictions, and Uncertainty*, 480 pp., John Wiley, Hoboken, N.J.

Johnes, P. J. (1996), Evaluation and management of the impact of land use change on the nitrogen and phosphorus load delivered to surface waters: The export coefficient modelling approach, *J. Hydrol.*, *183*(3–4), 323–349.

Kauffman, L. J., and F. H. Chapelle (2010), Relative vulnerability of public supply wells to VOC contamination in hydrologically distinct regional aquifers, *Ground Water Monit. R.*, *30*(4), 54–63.

Konikow, L. F. (2011), The secret to successful solute-transport modeling, *Ground Water*, *49*(2), 144–159, doi:10.1111/j.1745-6584.2010.00764.x.

Korom, S. F. (1992), Natural denitrification in the saturated zone—a review, *Water Resour. Res.*, *28*(6), 1657–1668.

Lasdon, L. S., A. D. Waren, A. Jain, and M. Rather (1978), Design and testing of a generalized reduced code for nonlinear programming, *ACM T. Math. Software*, *4*(1), 34–50.

McMahon, P. B., and F. H. Chapelle (2008), Redox processes and water quality of selected principal aquifer systems, *Ground Water*, *46*(2), 259–271.

McMahon, P. B., J. K. Böhlke, and S. C. Christenson (2004a), Geochemistry, radiocarbon ages, and paleorecharge conditions along a transect in the central high plains aquifer, southwestern Kansas, USA, *Appl. Geochem.*, *19*(11), 1655–1686.

McMahon, P. B., J. K. Böhlke, and T. M. Lehman (2004b), Vertical gradients in water chemistry and age in the southern high plains aquifer, Texas, 2002, *U.S. Geol. Surv. Sci. Invest. Rep. 2004-5053*, 53 pp., U.S. Geol. Surv., Reston, Virginia.

McMahon, P. B., K. F. Dennehy, B. W. Bruce, J. J. Gurdak, and S. L. Qi (2007), Water-quality assessment of the high plains aquifer, 1999–2004, *U.S. Geol. Surv. Professional Paper 1749*, 136 p., U.S. Geol. Surv., Reston, Virginia.

McMahon, P. B., J. K. Böhlke, L. J. Kauffman, K. L. Kipp, M. K. Landon, C. A. Crandall, K. R. Burow, and C. J. Brown (2008a), Source and transport controls on the movement of nitrate to public supply wells in selected principal aquifers of the United States, *Water Resour. Res.*, *44*(4), W04401, doi:10.1029/2007WR006252.

McMahon, P. B., K. R. Burow, L. J. Kauffman, S. M. Eberts, J. K. Böhlke, and J. J. Gurdak (2008b), Simulated response of water quality in public-supply wells to land-use change, *Water Resour. Res.*, *44*, W00A06, doi:10.1029/2007WR006731.

Michel, R. L. (1989), Tritium deposition in the continental United States, *U.S. Geol. Surv. Water Resour. Invest. Rep. 89-4072*, p. 46., U.S. Geol. Surv. Water Resour., Reston, Virginia.

Nakamura, K., T. Harter, Y. Hirono, H. Horino, and T. Mitsuno (2004), Assessment of root zone nitrogen leaching as affected by irrigation and nutrient management practices, *Vadose Zone J.*, *3*(4), 1353–1366.

Nolan, B. T., and K. J. Hitt (2006), Vulnerability of shallow groundwater and drinking-water wells to nitrate in the United States, *Environ. Sci. Technol.*, *40*(24), 7834–7840.

Nolan, B. T., K. J. Hitt, and B. C. Ruddy (2002), Probability of nitrate contamination of recently recharged groundwaters in the conterminous United States, *Environ. Sci. Technol.*, *36*(10), 2138–2145.

Nolan, B. T., L. J. Puckett, L. Ma, C. T. Green, E. R. Bayless, and R. W. Malone (2010), Predicting unsaturated zone nitrogen mass balances in agricultural settings of the United States, *J. Environ. Qual.*, *39*, 1051–1065, doi:10.2134/jeq2009.0310.

Pionke, H. B., and J. B. Urban (1985), Effect of agricultural land-use on groundwater quality in a small Pennsylvania watershed, *Ground Water*, *23*(1), 68–80.

Postma, D., C. Boesen, H. Kristiansen, and F. Larsen (1991), Nitrate reduction in an unconfined sandy aquifer-water chemistry, reduction processes, and geochemical modeling, *Water Resour. Res.*, *27*(8), 2027–2045.

Puckett, L. J., A. J. Tesoriero, and N. M. Dubrovsky (2011), Nitrogen contamination of surficial aquifers-a growing legacy, *Environ. Sci. Technol.*, *45*, 839–844.

Robertson, W. D., B. M. Russell, and J. A. Cherry (1996), Attenuation of nitrate in aquitard sediments of southern Ontario, *J. Hydrol.*, *180*, 267–281.

Rodvang, S. J., and W. W. Simpkins (2001), Agricultural contaminants in Quaternary aquitards: A review of occurrence and fate in North America, *Hydrogeol. J.*, *9*(1), 44–59.

Ruddy, B. C., D. L. Lorenz, and D. K. Mueller (2006), County-level estimates of nutrient inputs to the land surface of the conterminous United States, 1982–2001, *U.S. Geol. Surv. Sci. Invest. Rep. 06-5012*, 17 pp., U.S. Geol. Surv. Sci., Washington, D.C.

Singleton, M. J., B. K. Esser, J. E. Moran, G. B. Hudson, W. W. McNab, and T. Harter (2009), Saturated zone denitrification: Potential for natural attenuation of nitrate contamination in shallow groundwater under dairy operations, *Environ. Sci. Technol.*, *41*, 759–765.

Soil Conservation Service (1992), *Agricultural Waste Management Field Handbook, Chapt.* 4, 753 pp., U.S. Government Printing Office, Washington, D.C.

Spalding, R. F., and M. E. Exner (1993), Occurrence of nitrate in groundwater—a review, *J. Environ. Qual.*, *22*(3), 392–402.

Starn, J. J., A. C. Bagtzoglou, and G. A. Robbins (2010), Using atmospheric tracers to reduce uncertainty in groundwater recharge areas, *Ground Water*, *48*(6), 858–868.

Tesoriero, A. J., and L. J. Puckett (2011), O_2 reduction and denitrification rates in shallow aquifers, *Water Resour. Res.*, *47*, W12522, doi:10.1029/2011WR010471.

Tesoriero, A. J., and F. D. Voss (1997), Predicting the probability of elevated nitrate concentrations in the Puget Sound Basin: Implications for aquifer susceptibility and vulnerability, *Ground Water*, *35*(6), 1029–1039.

Tesoriero, A. J., D. A. Saad, K. R. Burow, E. A. Frick, L. J. Puckett, and J. E. Barbash (2007), Linking ground-water age and chemistry data along flow paths: Implications for trends and transformations of nitrate and pesticides, *J. Contam. Hydrol.*, *94*(1–2), 139–155.

Vogel, J. C. (1967), Investigation of groundwater flow with radiocarbon, in *Isotopes in Hydrology*, pp. 355–369, International Atomic Energy Agency, Vienna, Austria.

Vogel, J. C., A. S. Talma, and T. H. E. Heaton (1981), Gaseous nitrogen as evidence for denitrification in groundwater, *J. Hydrol.*, *50*(1–3), 191–200.

Weissmann, G. S., Y. Zhang, E. M. LaBolle, and G. E. Fogg (2002), Dispersion of groundwater age in an alluvial aquifer system, *Water Resour. Res.*, *38*(10), 1198, doi:10.1029/2001WR000907.

Welch, H. L., C. T. Green, and R. H. Coupe (2011), The fate and transport of nitrate in shallow groundwater in northwestern Mississippi, *Hydrogeol. J.*, *19*(6), 1239–1252, doi:10.1007/s10040-011-0748-8.

Wriedt, G., and M. Rode (2006), Modelling nitrate transport and turnover in a lowland catchment system, *J. Hydrol.*, *328*(1–2), 157–176.

Zhang, H., and K. M. Hiscock (2010), Modelling the impact of forest cover on groundwater resources: A case study of the Sherwood Sandstone aquifer in the East Midlands, UK, *J. Hydrol.*, *392*(3–4), 136–149.

B. A. Bekins, C. T. Green, and L. Liao, National Research Program, U. S. Geological Survey, 345 Middlefield Rd., Menlo Park, CA 94025, USA. (lliao@usgs.gov)

J. K. Böhlke, National Research Program, U. S. Geological Survey, 12201 Sunrise Valley Dr., Reston, VA 21092, USA.